

# NOVEL HYDROGELS FOR WOUND CARE APPLICATIONS

by

Yağmur Baş

B.S., Chemistry, Boğaziçi University, 2016

Submitted to the Institute for Graduate Studies in  
Science and Engineering in partial fulfillment of  
the requirements for the degree of  
Master of Science

Graduate Program in Chemistry

Boğaziçi University

2020

*Dedicated to Sevim, Zeynep, Mercan and all the strong women out  
there*

## ACKNOWLEDGEMENTS

First of all, I would like to express my sincere appreciation and gratitude to my thesis supervisor Prof. Amitav Sanyal. It has been an honour for me to be one of his students. His excellent guidance, deep knowledge of chemistry, passion for science and creativity had a big impact on me in addition to his contributions which I will preserve for a lifetime.

I would like to thank Prof. Rana Sanyal for her supervision. Her values, dedication and scientific work is a role model for every young woman who want to realize themselves in science and produce for their country.

My most sincere thanks comes for my family, my dear mother Zeynep, lovely grandmother Sevim and my beloved sister Mercan for their endless support. I also would like to thank my aunt Asuman & uncle Rıza Güven and my cousin İlayda Atak for their moral support throughout my entire life. They truly mean everything to me in life and this thesis would not exist if it was not for my family.

I deeply appreciate İsmail Altınbaşak for his contribution on this project. It was a pleasure to share the joy of research with all people in the lab. I learned great things from them while sharing unforgettable memories. I love them all.

I am grateful to each member of Yıldırım family for supporting me to do international research. Hicran, Zafer, Diren, Nine, Simon, Pancu, Lara and especially- Ümit Yıldırım deserves my best appreciation. I also would like to thank Dr. Jochen Niemeyer and Frescilia-Octa Simolin for everything they have taught me during my time in Germany.

I would like to thank Canan Arslan Güler for being my best friend. Her support and friendship was extremely valuable. I also would like to express my appreciation and love for my dear friends Canberk Çetin, İlke Albar, Erman Kayhan, Berkay Mordoğan, Duru Kadioğlu, Talitha Smit, Burak Erkek and Korhan Erişir.

I would also like to convey thanks to Bogazici University Research Projects for the funding of this research with project code 14825.

## ABSTRACT

### NOVEL HYDROGELS FOR WOUND CARE APPLICATIONS

Hydrogels are cross-linked, three-dimensional hydrophilic polymeric networks. They possess similarity in structure to the soft tissue in the body, thus have found a great number of applications as biomaterials. For wound care applications, hydrogels are considered to be new forms of wound dressings. Hydrogels with designed properties can act as a barrier for wounds while fastening the healing process. They can also cargo macromolecules encapsulated within their structure that are necessary for wound regeneration and protection.

The aim of this thesis is to synthesize redox responsive hydrogels that can be applied as wound care materials. Said hydrogels were designed to obtain a tissue regeneration triggering, non-cytotoxic and on-demand degradable hydrogel dressing to avoid disturbance of tissue while the material is physically removed. To do so, hyaluronic acid, a natural polymer constituent of human soft tissue, was modified with furan groups to construct hydrogels through reaction with a maleimide and disulfide functional group containing redox-responsive PEG-based crosslinker by Diels-Alder cycloaddition. The stimuli responsive degradation features are tuned by varying the amount of crosslinker in hydrogels. The change of porosity and disulfide concentration was expected to effect the degradation rates. It was demonstrated that hydrogels with higher crosslinking density exhibited greater strength, along with longer degradation times. All hydrogels exhibited high swelling capacity. To examine the passive and on-demand delivery of tissue regenerative macromolecules from this system, a model protein, namely, FITC-BSA was encapsulated within the hydrogels. The release of these biomolecules were investigated in PBS (pH=7.4), in absence and presence of the reducing agent DTT, to observe the passive and on-demand release profiles. Importantly, complete dissolution of the hydrogel was accomplished under mild conditions upon exposure to a solution containing the reducing agent.

## ÖZET

# YARA TEDAVİSİ İÇİN ÖZGÜN HİDROJEL SİSTEMLER

## TABLE OF CONTENTS

<b>ACKNOWLEDGEMENTS .....</b>	<b>iv</b>
<b>ABSTRACT.....</b>	<b>vi</b>
<b>ÖZET .....</b>	<b>vii</b>
<b>TABLE OF CONTENTS .....</b>	<b>vii</b>
<b>LIST OF FIGURES .....</b>	<b>x</b>
<b>LIST OF TABLES .....</b>	<b>xii</b>
<b>LIST OF ACRONYMS/ABBREVIATIONS .....</b>	<b>xiii</b>
<b>1. INTRODUCTION .....</b>	<b>1</b>
<b>1.1. Hydrogels .....</b>	<b>1</b>
1.1.1. Hydrogels As Wound Care Materials.....	3
1.1.2. On-Demand Degradable Hydrogels.....	4
<b>1.2. Hyaluronic Acid.....</b>	<b>6</b>
1.2.1. Structure.....	6
<b>1.3. Click Chemistry .....</b>	<b>12</b>
1.3.1. Diels-Alder Cycloaddition Reaction.....	14
<b>2. AIM OF THE STUDY.....</b>	<b>16</b>
<b>3. EXPERIMENTAL .....</b>	<b>17</b>

<b>3.1. Materials .....</b>	<b>17</b>
<b>3.2. Instrumentation .....</b>	<b>17</b>
<b>3.3. Furan Modification of Hyaluronic Acid.....</b>	<b>18</b>
<b>3.4. Synthesis of Bismaleimide Crosslinker .....</b>	<b>18</b>
3.4.1. Synthesis of Furan Protected Maleimide Alcohol .....	18
3.4.2. Synthesis of PEG-Bisacid .....	18
3.4.3. Synthesis of Furan Protected Bismaleimide .....	19
3.4.4. Synthesis of PEG-Bismaleimide Crosslinker .....	20
<b>3.5. Synthesis of Redox Responsive HA Hydrogels .....</b>	<b>20</b>
<b>3.6. Characterization of Redox Responsive HA Hydrogels .....</b>	<b>21</b>
3.6.1. Gelation Yields .....	21
3.6.2. Swelling Profiles.....	21
3.6.3. SEM Images of the Microstructures .....	21
3.6.4. Rheological Studies .....	22
<b>3.7. Degradation Studies .....</b>	<b>22</b>
3.7.1. Visual Degradation Studies .....	22
3.7.2. Rheological Investigation of Stability in PBS .....	22
3.7.3. Rheological Investigation of Degradation in DTT .....	23
<b>3.8. Encapsulation of FITC-BSA within the Hydrogels.....</b>	<b>23</b>
<b>3.9. Release of FITC-BSA from HG1 through Passive Diffusion and Redox     Responsive Degradation .....</b>	<b>23</b>
<b>4. RESULTS AND DISCUSSION .....</b>	<b>25</b>
<b>4.1. Synthesis and Characterization of Furan Modified Hyaluronic Acid .....</b>	<b>25</b>

<b>4.2. Synthesis and Characterization of PEG-Bisacid .....</b>	<b>26</b>
<b>4.3. Synthesis and Characterization of Furan-Protected Bismaleimide Crosslinker .....</b>	<b>28</b>
<b>4.4. Synthesis and Characterization of Bismaleimide Crosslinker .....</b>	<b>29</b>
<b>4.5. Synthesis and Characterization of Redox Responsive Hydrogels .....</b>	<b>31</b>
<b>4.6. Scanning Electron Microscope Images of Hydrogels.....</b>	<b>33</b>
<b>4.7. Swelling Profiles .....</b>	<b>33</b>
<b>4.8. Rheological Properties .....</b>	<b>34</b>
<b>4.9. Degradation Profiles .....</b>	<b>36</b>
<b>4.10. Diffusional and On-Demand Release Profiles of FITC-BSA from HG1.....</b>	<b>41</b>
<b>5. CONCLUSIONS .....</b>	<b>43</b>
<b>REFERENCES.....</b>	<b>44</b>
<b>APPENDIX A: ADDITIONAL DATA .....</b>	<b>50</b>
<b>APPENDIX B: COPYRIGHTS .....</b>	<b>52</b>

## LIST OF FIGURES

Figure 1.1. Types of stimuli responsive hydrogels and application areas [5].	1
Figure 1.2. a) Conventional polyester plasters b) Commercially available transparent dressing 3M Tegaderm.	4
Figure 1.3. Reduction of disulfide to thiols in presence of DTT.	5
Figure 1.4. The synthesis of the DA crosslinked hydrogel [24]. Degradation in 21 mM	6
Figure 1.5. The chemical structure of HA.	7
Figure 1.6. HA receptors and degradation times through the human body [29].	7
Figure 1.7. Available modification chemistry on the carboxylic acid and primary alcohol groups of HA [26].	8
Figure 1.8. HA hydrogels crosslinked with Huisgen click reaction [40].	9
Figure 1.9. The controlled BMP-2 release profiles from HA hydrogels [41].	10
Figure 1.10. The controlled BMP-2 release profiles from HA hydrogels. [41]	10
Figure 1.11. HA hydrogel gelation via Diels-Alder click reaction [44].	11
Figure 1.12. Main categories of click reactions [48].	12
Figure 1.13. Injectable HA hydrogel synthesis via click chemistry [51].	13
Figure 1.14. Synthesis of 3D bio-printable HA hydrogel via radical click reaction [52].	14
Figure 1.15. Reversible DA reaction between furan (diene) and maleimide (dienophile) [55].	15
Figure 2.1. Schematic representation of the project.	16
Figure 4.1. Synthesis of furan modified hyaluronic acid.	25
Figure 4.2. <sup>1</sup> H NMR spectrum of the furan modified hyaluronic acid.	26
Figure 4.3. Synthesis of PEG-Bisacid.	27

Figure 4.4. $^1\text{H}$ NMR spectra of PEG-Bisacid in $\text{CDCl}_3$ .....	27
Figure 4.5. $^1\text{H}$ NMR spectra of PEG-Bisacid in $\text{CDCl}_3$ with $\text{D}_2\text{O}$ . ....	28
Figure 4.6. Synthesis of Furan Protected PEG-Bismaleimide.....	29
Figure 4.7. $^1\text{H}$ NMR spectrum of Furan Protected PEG-Bismaleimide.....	29
Figure 4.8. Synthesis of Bismaleimide Crosslinker.....	30
Figure 4.9. $^1\text{H}$ NMR spectrum of Bismaleimide Crosslinker.....	30
Figure 4.10. Synthesis of redox-responsive HA hydrogel.....	31
Figure 4.11. A) Inverted tube and B) swollen state images of HG1.....	32
Figure 4.12. SEM images of a) HG1, b) HG2 and c) HG3. Scale bar: 200 $\mu\text{m}$ . ....	33
Figure 4.13. Swelling ratios of HG1, HG2 and HG3. ....	34
Figure 4.14. Visual images of HG3 in their A) dried and B) swollen states. ....	34
Figure 4.15. Frequency Sweep (Right) and Amplitude Sweep (Left) tests of HG1.....	35
Figure 4.16. Frequency Sweep (left) and Amplitude Sweep (right) tests of HG2. ....	35
Figure 4.17. Frequency Sweep (left) and Amplitude Sweep (right) tests of HG3. ....	36
Figure 4.18. Combined Frequency Sweep Tests of HG1, HG2 and HG3.....	36
Figure 4.19. Visual stability of FITC encapsulated HG1 encapsulates images in only PBS at rt.....	37
Figure 4.20. Visual degradation of HG1 in 5 mM DTT at rt.....	37
Figure 4.21. Stability of HG1, HG2, and HG3 in PBS.....	38
Figure 4.22. Time Sweep Test of HG1 in 10 mM DTT. ....	39
Figure 4.23. Time Sweep Test of HG2 in 10 mM DTT. ....	39
Figure 4.24. Time Sweep Test of HG3 in 10 mM DTT. ....	40
Figure 4.25. Redox responsive degradation of HG1, HG2 and HG3 in rheometer as a function of time.....	40
Figure 4.26. Release of FITC-BSA from HG1 in PBS and upon the addition of 50 mM DTT. .....	42
Figure A.1. GPC plot of PEG. ( $M_w=4\text{kDa}$ ).....	50
Figure A.2. GPC plot of furan protected bismaleimide crosslinker. ....	51
Figure A.3. GPC plot of bismaleimide crosslinker.....	51

## LIST OF TABLES

Table 4.1. Conversion of hydrogels with different crosslinking densities. ....	32
Table A.1. GPC results of the crosslinker .....	32

**LIST OF ACRONYMS/ABBREVIATIONS**

D <sub>2</sub> O	Deuterium Oxide
DA	Diels Alder
DCC	(N,N Dicyclohexylcarbodiimide)
DMAP	4-Dimethylaminopyridine
DMTMM	(4-(4,6-dimethoxy-1,3,5-triazin-2-yl)-4-methyl-morpholinium chloride)
DTT	1,4-dithiothreitol
ECM	Extracellular Matrix
FM	Furan Maleimide
F/M	Furan to Maleimide ratio
G'	Storage Modulus
G''	Loss Modulus
GAG	Glycosaminoglycan
GPC	Gel Permeation Chromatography
GSH	Glutathione
FITC-BSA	Fluorescence labeled Bovine Serum Albumin
HA	Hyaluronic Acid
NMR	Nuclear Magnetic Resonance
NP	Natural Polymers
MES	2-(N-morpholino)ethanesulfonic acid
M <sub>n</sub>	Number Average Molecular Weight
NMR	Nuclear Magnetic Resonance
PBS	Phosphate Buffer Saline
PEG	Poly(ethylene glycol)
rDA	Retro Diels-Alder reaction
rt	Room Temperature
SEM	Scanning Electron Microscope
SH	Thiol group
SP	Synthetic Polymers
THF	Tetrahydrofuran
UV-vis	Ultraviolet visible region

# 1. INTRODUCTION

## 1.1. Hydrogels

Hydrogels are cross linked hydrophilic 3D polymer networks with high water absorption ability and they can retain large volumes of liquids in their swollen state [1]. They exhibit a highly porous structure which can be tuned by controlling the crosslinking density and their porosity permits loading of cells, drugs, proteins into the gel matrix with spatially and temporally controlled release of these agents [2]. The transfer process can occur via simple diffusion or stimuli-responsive fashion where the trigger of an external change in the environment results in a response of the system. Some examples to such situations are thermoresponse [3], photoresponse [4] or redox-response [5].

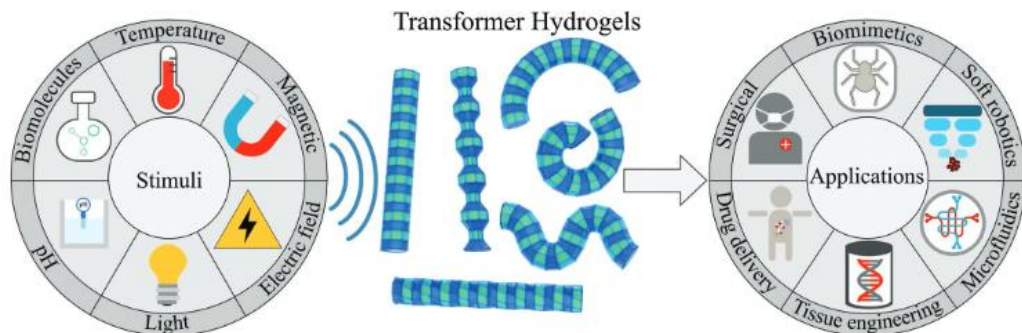


Figure 1.1. Types of stimuli responsive hydrogels and application areas [5].

The porous architecture and the high water absorption ability of hydrogels promotes biocompatibility. With their soft consistent texture, they possess structural resemblance to the mammalian living tissue which is consisted of a variety macromolecule residents with gaps in between. [6], [7] The biodegradability of these porous materials can be designed using enzymatic, hydrolytic and environmental pathways [8]. These advantageous features make hydrogels promising candidates for regenerative biomaterials and drug delivery systems.

Hydrogels can be classified depending on their synthesis route and crosslinking bond type. The synthesis of polymeric hydrogels are mainly achieved either by polymerization of monomers which are named as synthetic polymers (SP) or by modification of readily occurred polymers that are natural polymers (NP). Incorporating hydrophilic monomers in SP based hydrogel structures yields enhanced water uptake, drug/molecule loading and a better diffusional release. Two examples of these monomers are hydroxy ethylmetacrylate (HEMA) and ethylene glycol dimethacrylate (EGDMA) [9]. In biomedical applications, poly(ethyleneglycol) (PEG) moiety bearing polymers are widely used because PEG contains a less toxic, hydrophilic, biocompatible and easily functionalizable structure [10].

The crosslinking of polymers is achieved by either using physical interactions such as ionic interactions, H-bonding and hydrophobic interactions or via covalent bonds that are chemical bonds. In chemically crosslinked hydrogels, polymers are covalently bonded to each other and the network is stabilized with strong covalent bonds thus these gels exhibit greater stability and enhanced mechanical properties [11], [12]. The polymer constituents are either synthetically produced via polymerization techniques or naturally produced, as well as the combination of the said two.

Mostly, SP enables chemists to obtain well defined or desired structures with further modification abilities on the polymer backbone. However, most of the SP based hydrogels cannot bear excellent biocompatibility and they often contain by-products left in the hydrogel matrix caused by the synthesis process or degradation of the polymer backbone. In addition to SP, modifiable NP also allow to derive new materials with desired properties by functionalizing the available sites on the NP backbone. NP that are fundamental parts of human tissue such as collagen, hyaluronan and chondroitin sulfate hold the power of excellent biocompatibility, enhanced water solubility, immune compatibility and high cellular uptake ability readily within their structure. These macromolecules are extensively used in tissue regeneration and wound care applications to create hydrogel scaffolds with novel properties [13].

### **1.1.1. Hydrogels As Wound Care Materials**

Wound is the breakage in the living tissue that occurs with any reason. Immediately after an injury, the healing at the site of lesion starts with the response of body [14]. As an external source during the restoration process, the wound site is wrapped with biomaterials to avoid infections and protect it from physical strikes. These materials to care the wound are called as dressings.

Conventional type of medical dressings are the cotton or polyester dressings which act as a barrier in between the site of wound and the surrounding space. The care process is repetitive until the tissue is fully regenerated and a major drawback of commercial dressings is they stick on the wound surfaces, especially when burn wounds are considered [15]. During the replacement with new patches, the freshly epithelized tissue at ongoing healing process is disturbed or ruined, the regeneration mechanism is blocked and as a mechanical consequence patients end up experiencing a considerable amount of pain [16]. The stated situations are challenges to overcome with emerging dressing technologies.

In recent years, hydrogels as wound dressings have become the subject of interest to obtain better quality materials to meet the requirements of an ideal wound care process [17]. They can act as flexible yet firm enough mechanically protecting barriers. The absorption appetite of these materials results in enhanced swelling abilities and a moist environment, where the moist is associated with fastened healing, decreased pain and less scar formation. While swelling takes place, retaining the exudates secreted from the site of wound and present pathogens results in enhanced infection control [15]. Retaining the exudates is also a trigger for the migration of healthy epithelial cells which are located at the deeper levels of the tissue, thus accelerates the healing [18]. Another advantage of hydrogels might be the transparency which allows medical staff to examine the situation of the wound through the patch, already before the removal.

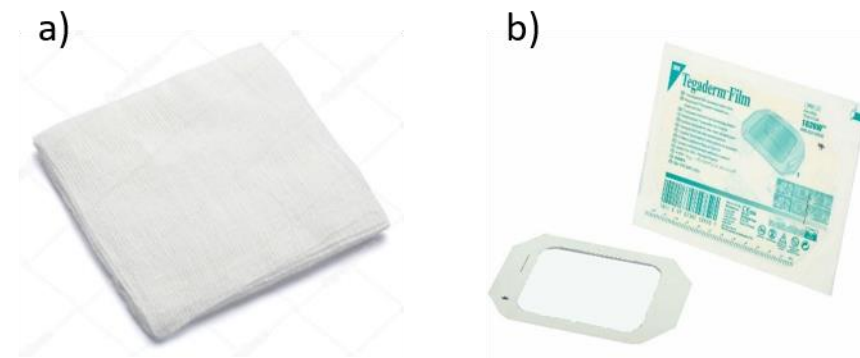


Figure 1.2. a) Conventional polyester plasters b) Commercially available transparent dressing 3M Tegaderm. [20]

Wound regeneration also greatly benefits from hydrogel dressings since they can perform the topical delivery of encapsulated or covalently bonded agents within their structure. Using this speciality, M. Chen and coworkers designed a collagen based hydrogel dressing loaded with antimicrobial chlorhexidine acetate together with fibroblast growth factor microspheres [19]. The authors developed this system to successfully deliver mentioned protection and regeneration cargos while mechanically protecting the site of wound. To specifically emphasize the effect of glycosaminoglycan (GAG) based wound dressings such as hyaluronic acid hydrogels on tissue re-epithelization, K.R. Kirker *et al.* compared a set of HA and CS hydrogels with Tegaderm™, which is a non-GAG commercially available transparent wound dressing [20].

### 1.1.2. On-Demand Degradable Hydrogels

On-demand degradable hydrogels exhibit a manageable dissolution profile whenever the degradation is desired. For this purpose, a chemical bond susceptible to cleavage via hydrolysis or enzymatic degradation is inserted within the hydrogel network [21]. In such systems, with the incorporation of the degradation agents, the hydrogel can shatter and washed away from applied surface. As far as the burn wound care is considered, any physical intervention such as pulling away the dressing can be prevented and the recruitment of tissue can be preserved by using on demand degradation strategy.

r-DA, r-Michael addition, thiol-thioester and thiol-disulfide exchange reactions are some of the tools to acquire on demand degradable hydrogels. For r-DA reactions, usually high temperatures are necessary to break down the cycloadduct and the dissolution rate is slow. Said disadvantages makes r-DA an unpractical way for obtaining a fast on-demand degradability profile and to apply such high temperatures on patients is not possible. Thiol-disulfide exchange reaction is widely used redox reaction with  $S_N2$  type mechanism where a thiolate anion ( $RS^-$ ) attacks one of the sulfur atoms present in the disulfide bond to produce a new disulfide bond [22]. As a result of the cleavage, a free thiolate ion is formed and reduced to a thiol. A well-known reducing agent secreted in mammalian tissue for disulfide reduction is L-glutathione (GSH) [23]. There also exists non-mammalian, stronger reducing agents such as dithiothreitol (DTT) which might yield to more rapid degradation of disulfide bonds. (Figure 1.3)

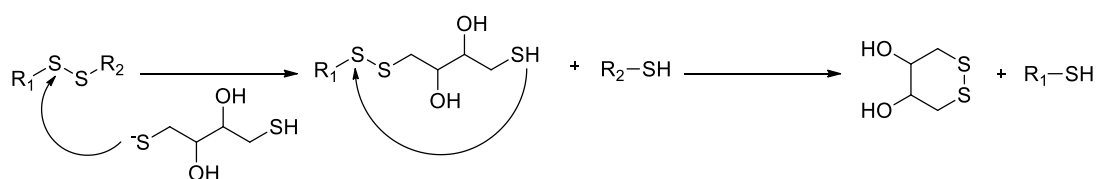


Figure 1.3. Reduction of disulfide to thiols in presence of DTT.

In 2016, Sanyal *et al.* have synthesized a redox responsive, biodegradable hydrogel via DA reaction for controlled protein release purposes using on demand degradation strategy [24]. (Figure 1.4.) Degradation profiles via the cleavage of disulfide bonds in the presence of DTT are studied to prove that these hydrogels performed on demand degradation while carrying out the controlled release of fluorescence labeled bovine serum albumin (FITC-BSA).

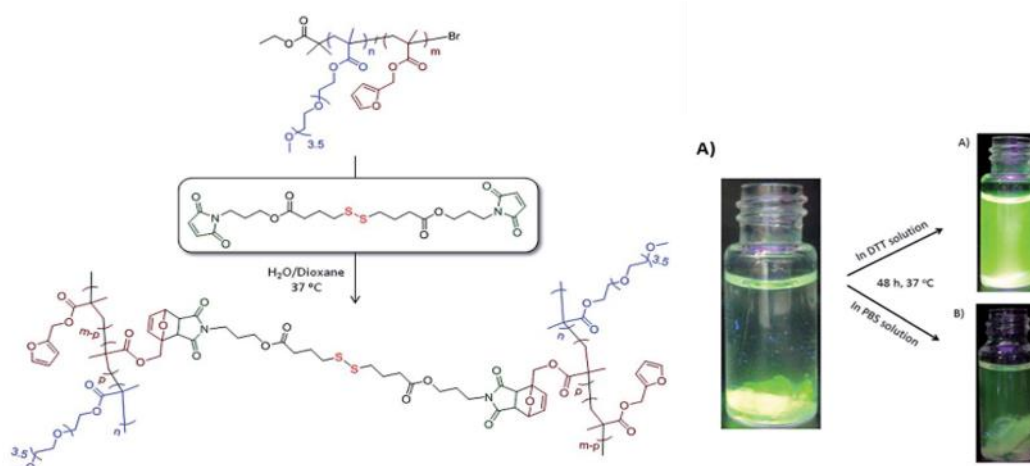


Figure 1.4. The synthesis of the DA crosslinked hydrogel [24]. Degradation in  $21\text{ mM DTT}$  [24].

## 1.2. Hyaluronic Acid

### 1.2.1. Structure

The extracellular matrix (ECM) is the mixed domain of miscellaneous macromolecules that are organized in a tissue or cell specific fashion. Collagen, laminin, fibronectin can be mentioned as the major members of these macromolecules [25]. When said protein, glycoprotein and proteoglycan macromolecules gather together in various defined morphologies, they provide necessary environment for cellular signaling and formation of a variety of different tissue types.

Hyaluronic acid (HA) is an immune neutral polysaccharide (MW:  $100\text{--}8000\text{ kDa}$ ) contained in the ECM of the human body, consisted of alternating units of repeating disaccharide  $\beta\text{-}1,4\text{-D-glucuronic acid}\text{-}\beta\text{-}1,3\text{-N-acetyl-D-glucosamine}$  [26].

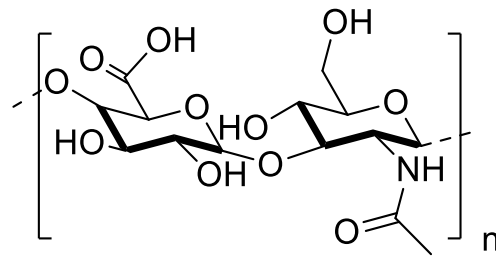


Figure 1.5. The chemical structure of HA.

Being one of the essential components of ECM, HA is found all throughout the mammalian body. It is biocompatible and reveals low levels of immune response [27]. HA is also involved in activities of cellular signaling, wound healing, morphogenesis, angiogenesis and matrix organization [28]. The cellular interaction with HA is expedited by CD44 and RHAMM receptors and it is rapidly degraded in body via an enzyme, named hyaluronidase, with half-lives ranging from hours to days depending on the type of the tissue [10]. (Figure 1.6.)

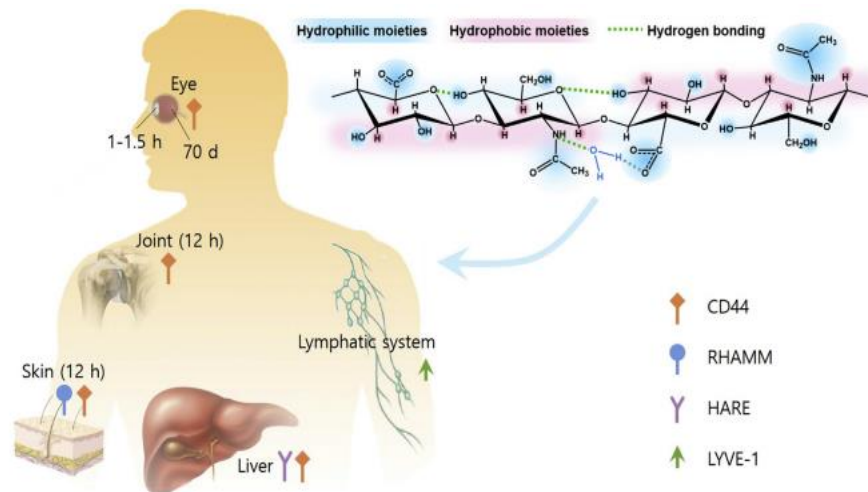


Figure 1.6. HA receptors and degradation times through the human body [29].

When medical application is intended, the fast degradation and clearance profile of HA requires covalent bonding for enhanced stability of the material. HA can readily get chemically and physically modified with different chemical groups by means of the

glucuronic acid carboxylic acid group and primary hydroxyl groups in its structure [11]. Thus, HA derived materials with desired stability and mechanical properties can be synthesized. In addition, its importance in ECM composition, biodegradable structure and modification feasible nature makes HA an excellent candidate for wound healing, tissue regeneration and sustained release applications [30]. HA has been extensively exploited to synthesize numerous biomedical systems such as hydrogels, nanogels [31], nanoparticles [32] and semi synthetic fibers [33].

One of the key HA derived biomaterials are the hydrogels. HA based hydrogels have diverse application areas such as creating scaffolds for in vitro tissue growth or in vivo tissue regeneration [8]. They are also used as tools for the controlled release of drugs or essential biological molecules like growth factors. Over the past years, a variety of HA based hydrogels are designed to carry hydrophobic drugs [34], cartilage tissue engineering [35], dural repair [36], bone regeneration [37] and act as central neural tissue scaffolds [38].

Mostly taking place at the carboxylic acid site, chemical modifications on hyaluronic acid enables them to further give gelation when a crosslinker is present. Available sites on hyaluronic acid can be modified with various different groups such as thiols, hydrazides, glycidyl methacrylates, tyramines and many more.

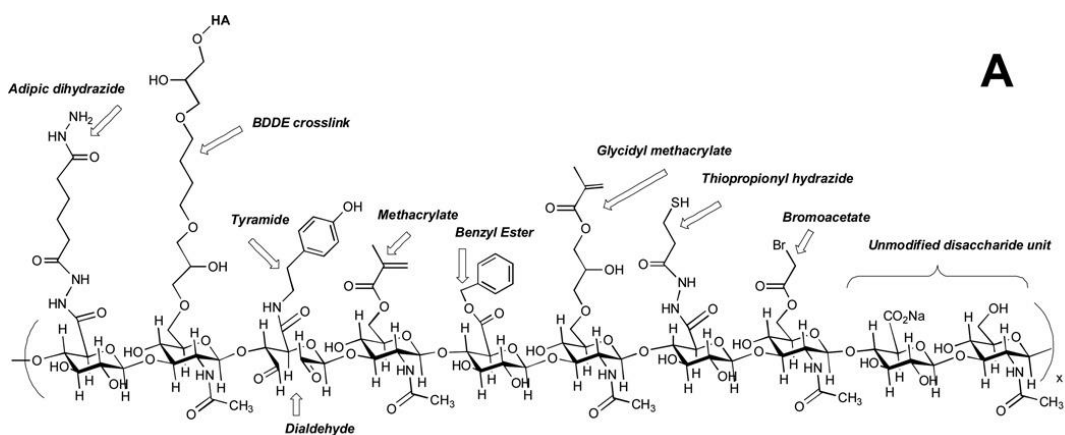


Figure 1.7. Available modification chemistry on the carboxylic acid and primary alcohol groups of HA [26].

For example, in 2003, X. Z. Shu *et al.* has synthesized a disulfide bearing HA-gelatin hybrid hydrogel scaffold by modifying the carboxylic acid sites via using 3,30-dithiobispropionic hydrazide. (DTP) The disulfide bonds in HA-DTP and gelatin-DTP were reduced to thiol groups with 1,4-dithiothreitol (DTT) to give crosslinking reaction at the thiol sites in the presence of air [39]. Said hydrogels were proven to be successful degradable scaffolds for fibroblast proliferation.

Again with hydrazide modification, Di Meo *et al.* applied Huisgen click reaction to obtain HA hydrogels to act as hydrophobic drug reservoirs [40]. HA is modified with propargylamine and azide terminals to react with each other via 1,3 dipolar cycloaddition reaction in the presence of Cu(I) catalyst to give faster gelation. The gels acted as scaffolds for successful yeast cell proliferation nevertheless this hydrogel was clinically cytotoxic due to Cu(I) residues.

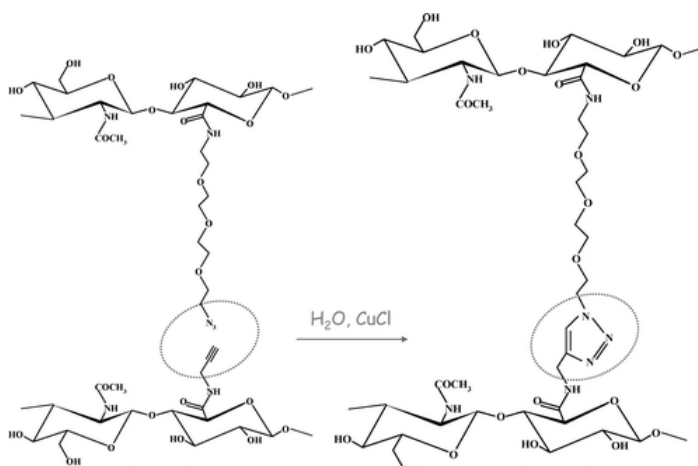


Figure 1.8. HA hydrogels crosslinked with Huisgen click reaction [40].

G. Bhakta *et al.* and coworkers have synthesized a HA based heparin bearing hydrogel system for the controlled release of Bone Morphogenesis Protein (BMP-2) in 2012 [41]. Thiol modified HA was crosslinked with PEG-diacrylate via Michael addition, which was notable to obtain UV free HA based hydrogels. (Figure 1.9)

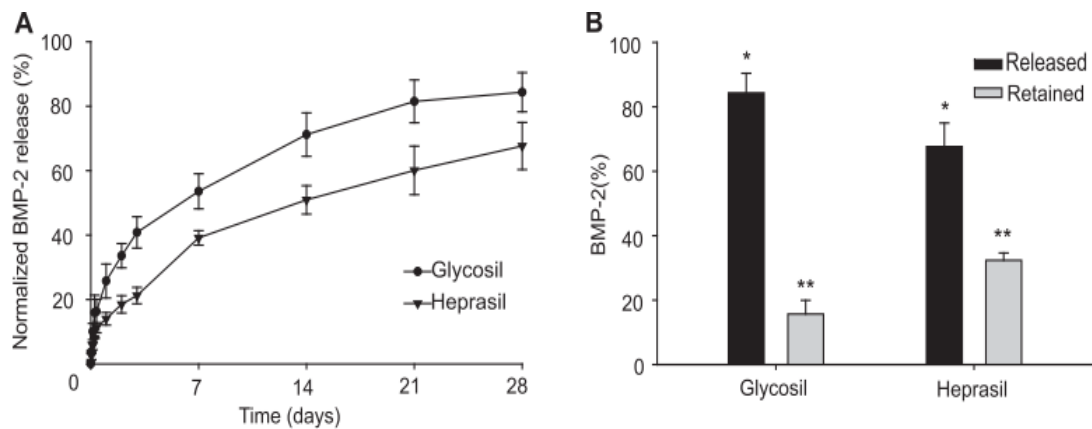


Figure 1.9. The controlled BMP-2 release profiles from HA hydrogels [41].

There also exists a variety of HA hydrogels synthesized using photo chemistry. Schmidt *et al.* has synthesized a photo crosslinked hydrogel using glycidyl methacrylate modified HA and acrylated 4-arm PEG to observe different protein release. The release profiles of BSA were studied depending on change of crosslinker density [42]. From there, S. Ibrahim and her group have synthesized a HA based hydrogel system via functionalizing the available primary alcohol sites with glycidyl methacrylate in 2011 [43]. Obtained derivatized HA was photo-crosslinked in the presence of UV light via the reaction between the acrylate sites. (Fig 1.10) In vivo studies showed that the GM-HA gel was biocompatible.

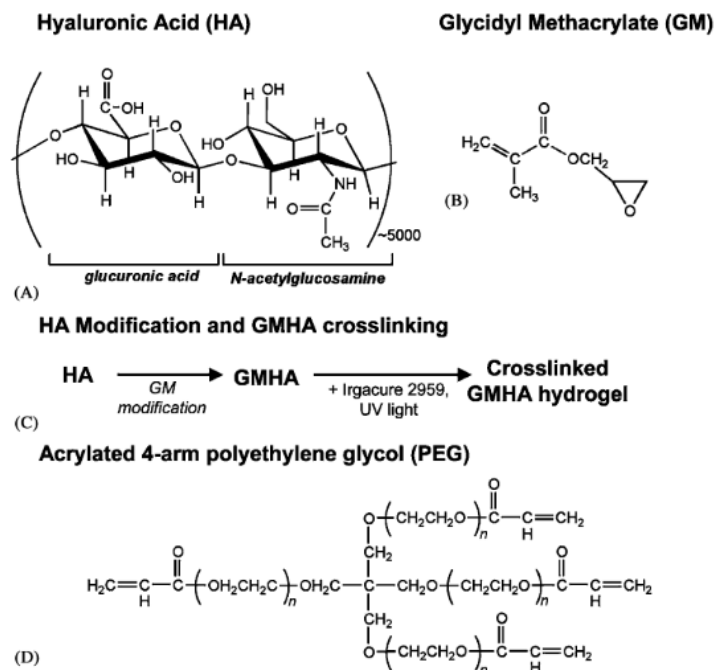


Figure 1.10. The controlled BMP-2 release profiles from HA hydrogels. [41]

Although there existed wide range of chemistry applied to obtain HA based hydrogels, new ways of catalyst free, clean and easier hydrogel synthesis was needed considering the biological applications. In that sense, the click chemistry available for HA systems was limited mainly with Michael addition and Huisgen addition which still required the use of Cu(I) catalyst. Regarding this limitation, in 2011, Shoichet *et al.* has gone beyond the traditional HA click chemistry and synthesized a HA hydrogel system crosslinked via DA cycloaddition reaction which took place between the furan functionalized HA and bismaleimide bearing crosslinker at pH 5.5 [44]. In their system, carboxylic acid sites on hyaluronic acid units were modified with furan groups where the catalyst free DA click reaction could further take place. (Figure 1.11) They showed a simple, one step and aqueous based hydrogel system which reduces the complexity of the synthesis and lacks of any coupling agents or catalyst, thus enhances its biocompatibility. Later on, in 2018, this system was improved by replacing furan groups with electron rich methylfurans to accelerate DA at pH 7.4 [45]. With faster gelation via DA at pH 7.4 resulted in a convenient system for 3D cell encapsulation purpose at physiological conditions.

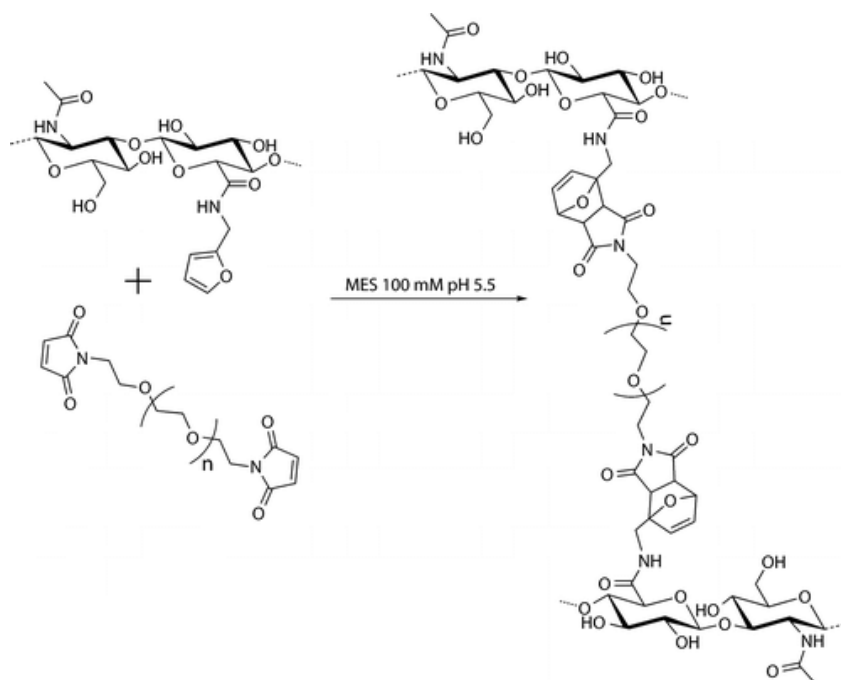


Figure 1.11. HA hydrogel gelation via Diels-Alder click reaction [44].

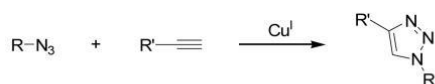
### 1.3. Click Chemistry

The term ‘‘click chemistry’’ was introduced by Sharpless and Finn in 2001 to define a set of reactions occurring in high yields under simple conditions with easily available starting materials [46]. Many of these reactions are also stereospecific and biorthogonal [47].

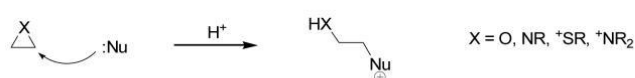
The essential requirements of click chemistry are orthogonal species reacting under mild conditions to yield a single stereospecific product with simple or even no purification process [48]. Click reactions can proceed without solvent and in water or the solvents are easily removed from the products. In general, the click reaction conditions fit with human physiological needs. Main classes of click reactions are cycloadditions, nucleophilic ring openings and carbon multiple bond additions.

#### Cycloadditions

Cu<sup>I</sup>-catalyzed Huisgen 1,3-dipolar cycloadditions of azides and alkynes

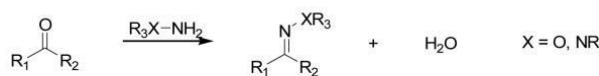


#### Nucleophilic Ring-Openings

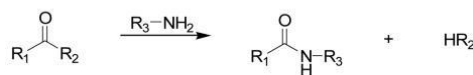


#### Non-Aldol Carbonyl Chemistry

Hydrazone/oxime ether formation



Amide/isourea formation



#### Carbon Multiple Bond Additions

Formation of various three-member rings



Certain Michael Additions



Figure 1.12. Main categories of click reactions [48].

When biomaterials are in consideration, click reactions are powerful tools to decrease toxicity while bringing out an easier and cleaner way of synthesis as well as bioapplication. Thus, click reactions have extensively been used in synthesizing biomaterials with novel properties. As an example, using 1,3 dipolar azide alkyne addition, Huang *et al.* have synthesized an Au-nanoparticle based colorimetric microbial ‘‘point of care’’ sensor inspired by bacterial metabolic pathways reducing  $\text{Cu}^{2+}$  to  $\text{Cu}^{+1}$ . [49]  $\text{Cu}^{+1}$  reduced by bacteria used to catalyze the Huisgen click reaction between azide and alkyne functionalized AuNPs which resulted in a change in color. In another work, Baharvand and coworkers put out a sustained local delivery system for mesenchymal stem cells (MSC) based on a PEG-SH and PEG-maleimide click crosslinked hydrogel [50]. The fast and self-driven click reaction allowed to design injectable hydrogels for the delicate delivery of stem cells.

Moreover, click chemistry has also widely applied in HA based hydrogels. Just recently, Moon Suk Kim and coworkers synthesized an injectable hydrogel by click reaction between tetrazine modified-HA and trans-cyclooctene modified HA for articular joints suffering rheumatoid arthritis which successfully prolonged the therapeutic activity [51].

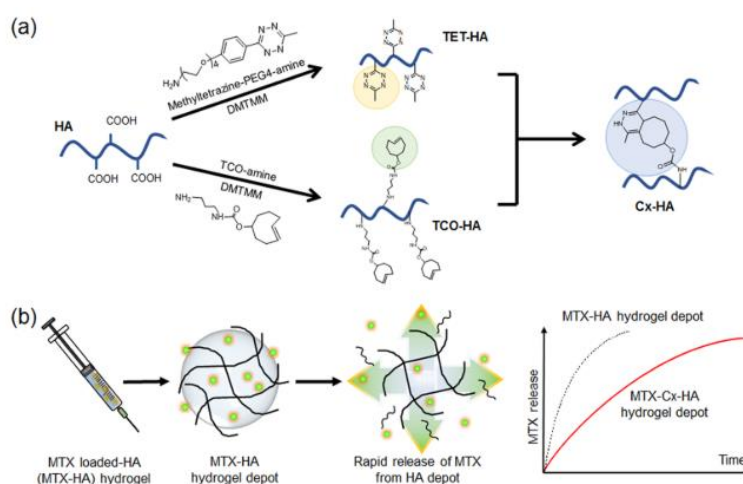


Figure 1.13. Injectable HA hydrogel synthesis via click chemistry [51].

In addition to reactions contained in Fig. 1.15, photoinitiated thiol-alkene reactions are another type of click reactions. Using this type of click reaction, Zhang *et al.* has come up with a double crosslinked 3D-bioprintable wound dressing for sustained drug release

purposes [52]. Thiol modified-HA were click crosslinked with HA-Metacrylate radicals created upon the addition of the initiator. Authors have shown that this system was highly cyto compatible for fibroblast proliferation and effective local transport of the Nafcillin, a  $\beta$ -lactam antibiotic, in addition to its 3D bioprintable characteristics.

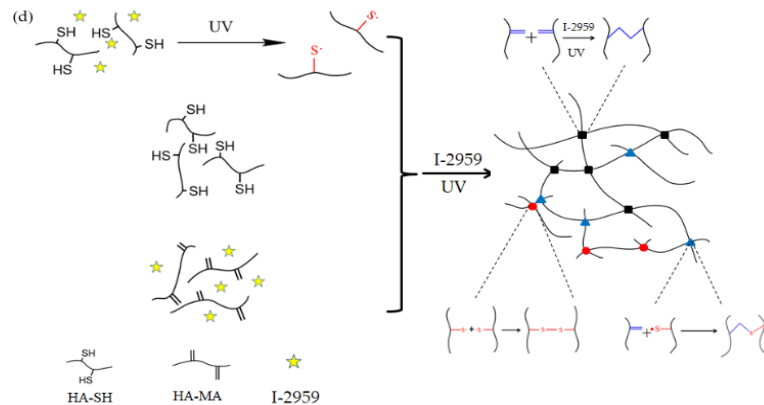


Figure 1.14. Synthesis of 3D bio-printable HA hydrogel via radical click reaction [52].

### 1.3.1. Diels-Alder Cycloaddition Reaction

The Diels-Alder (DA) is a single step, catalyst free and thermally reversible [4+2] cycloaddition reaction which takes place in between a conjugated diene and dienophile [53]. The thermo reversible nature of DA allows dissociation of the cycloadduct members back to their reactant states when necessary heat is given [54]. The reactive dienophile group prior to the functionalization or polymerization requires protection and the cycloreversion step at high temperatures might also cause decomposition of other materials within the synthesis [55]. Although there exists a variety of diene and dienophile pairs that holds the potential of DA click reaction, furan-maleimide is a widely exploited pair as this cycloadduct allows decoupling at relatively low temperatures.

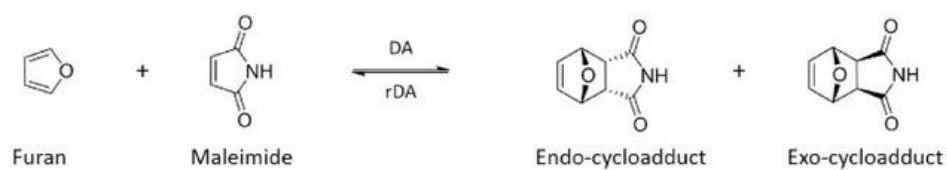


Figure 1.15. Reversible DA reaction between furan (diene) and maleimide (dienophile) [55].

By virtue of its thermo reversible and catalyst free click nature, the DA click chemistry is used to produce many HA hydrogels in as protein release systems, scaffolds for cell proliferation and controlled drug release agents. In 2015, Yu *et al.* have used DA crosslinked hydrogels to achieve spatiotemporal patterning by reacting furan-maleimide cyclohexene derivative with thiol modified molecules [56]. Hu and his group have used furan maleimide crosslinked HA hydrogels as a scaffold for vascular endothelial growth factor (VEGF) loaded nanoparticle release [57].

## 2. AIM OF THE STUDY

This study reports a novel method for the synthesis of a redox-responsive hydrogel system which can be used as a biocompatible and on-demand degradable dressing for wound care applications. For this reason, a highly biocompatible and tissue regenerative natural polymer, namely hyaluronic acid, is modified with furan groups and thereafter crosslinked with a PEG bearing bismaleimide crosslinker via Diels-Alder click reaction to yield hydrogels. For enhanced hydrophilicity purposes PEG moieties are integrated in the crosslinker structure, whereas redox-responsiveness is introduced through incorporation of disulfide linkages within the system. In order to investigate the change of microstructure and physical properties 3 hydrogels with different crosslinking densities were synthesized. By doing this, a change in the pore size together the tunability in degradation rates was expected to be achieved. Since this system was designed to be used as an on demand degradable wound dressing, the wash off of the dressing from the applied wound surface highly depended on the materials degradation features. After the investigation of hydrogels with different degradation profiles, FITC-BSA was physically encapsulated within these gels to further study the release profiles of therapeutics that are tissue regenerative agents as the wound care is considered. With the release studies it was aimed to run the controlled and on demand release of BSA, that is a model protein applied as a representative for tissue regenerative macromolecules.

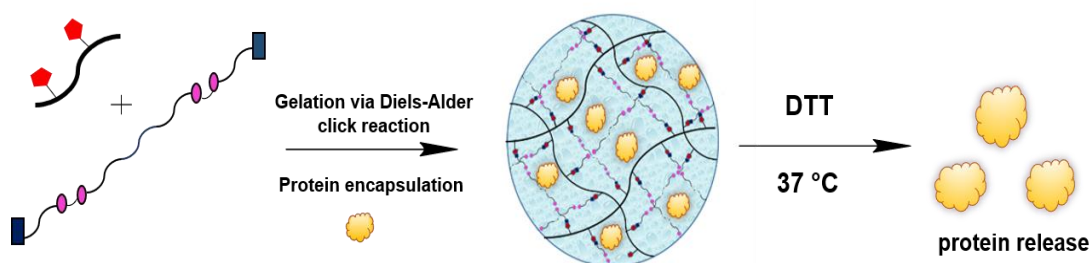


Figure 2.1. Schematic representation of the project.

### 3. EXPERIMENTAL

#### 3.1. Materials

Maleic Anhydride was purchased from Merck. Hyaluronic acid (HA) PRIMALHYAL 300 (Mw: 100-300 kDa) was purchased from Givaudan Products. Furan (>99%), 3-amino-1-propanol (>99%), 4,4'-dithiobutyric acid (>95%), 4-dimethylaminopyridine (DMAP), 4-(4,6-dimethoxy-1,3,5-triazin-2-yl)-4-methylmorpholinium chloride (DMTMM) (>96%) and fluorescein isothiocyanate conjugated bovine serum albumin (FITC-BSA) were purchased from Sigma-Aldrich. (Germany). *N,N'*-Dicyclohexylcarbodiimide (DCC), 1,4 dithiothreitol (DTT) (98%) and furfuryl amine (>99%) were purchased from Alfa-Aesar. (USA). 2-(*N*-morpholino)ethanesulfonic acid (MES) and MES Sodium salt were purchased from Glentham Life Sciences.

#### 3.2. Instrumentation

The furan modified HA and crosslinker characterization were carried out with <sup>1</sup>HNMR spectroscopy (Varian 400 MHz). The molecular weight of the PEG based bisacid and the crosslinker were determined by gel permeation chromatography (GPC) with (PSS-SDV, length/ID 8 \* 300 mm, 10 μm particle size) calibrated with polystyrene standards using a refractive-index detector. Dimethylacetamide (DMAC) was used as eluent at a flow rate of 1 mL/min at 30 °C.

The microstructures of the hydrogels were investigated with JEOL Neo Scope JCM-5000 scanning electron microscopy (SEM) instrument run at 10 kV. Rheological properties of the hydrogels were investigated with Anton PAAR MCR 302 rheometer where the results are measured as a function of *G'* (storage modulus) and *G''* (loss modulus) vs angular frequency and time. Fluorescein isothiocyanate (FITC)-labeled bovine serum albumin

(BSA) release from hydrogels was analyzed using Cary Varian 50 Scan UV/Vis spectrophotometer.

### **3.3. Furan Modification of Hyaluronic Acid**

Furan modified HA was synthesized according to the literature. [44] HA (Mw=200 kDa, 50 mg, 0.130 mmol COOH) was dissolved in MES buffer (5 mL, pH=5.5, 100 mM). (4-(4,6-dimethoxy-1,3,5-triazin-2-yl)-4-methyl-morpholinium chloride) (147 mg, 0.435 mmol) was added to this solution and reaction was stirred for 10 minutes at room temperature. Furfurylamine (43  $\mu$ l, 0.48 mmol) was added dropwise and the reaction was stirred at room temperature for 24 hours. The products were put in dialysis bag (12-14 kDa) and dialyzed against ultrapure water for 3 days for the purification. Product was obtained white porous solid after lyophilization.

### **3.4. Synthesis of Bismaleimide Crosslinker**

#### **3.4.1. Synthesis of Furan Protected Maleimide Alcohol**

The furan protected maleimide containing alcohol was synthesized according to the literature [58].

#### **3.4.2. Synthesis of PEG-Bisacid**

PEG-bisacid was synthesized through the esterification reaction between 4-4' dithiobutyric acid with poly(ethylene glycol). PEG (5 g, 1.25 mmol) was dried over 15 ml

of toluene for 3 times and stayed in high vacuum for 1 day until it was completely water free. DMAP (90 mg, 0.625 mmol) was added to this flask as solid and they were dissolved in 5 ml of anhydrous dichloromethane (DCM). 4-4' dithiobutyric acid (1.19 g, 5 mmol) and DCC (1.17 g, 5.625 mmol) were dissolved in 2.7 ml of anhydrous tetrahydrofuran (THF) in another flask and PEG-DMAP mixture was added dropwise to the said flask at 0 °C and stirred for 10 minutes at 0 °C under N<sub>2</sub>. Then the reaction stirred for 24 hours at room temperature under N<sub>2</sub>. For the purification of the PEG-Bisacid product, the solid N'-dicyclohexylurea residues were filtered and the reaction solvent was evaporated. The products were dissolved in 2 ml of DCM and were precipitated in 50 ml of ice cold diethyl ether four times repeatedly. The precipitated PEG-acid product was dried on high vacuum to be obtained as white solid powder. (4.2 g, yield= 76%, coupling efficiency=93%). <sup>1</sup>H NMR (CDCl<sub>3</sub>) δ (ppm): 4.23 (t, 4H), 3.85-3.35 (360H), 2.84 (s, 4H), 2.74 (t, 8H), 2.47 (m, 8H), 2.02 (m, 8H).

### 3.4.3. Synthesis of Furan Protected Bismaleimide

In a flask, the dried PEG-Bisacid (600 mg, 0.134 mmol) was dissolved in anhydrous DCM (0.8 mL). DCC was dissolved in anhydrous DCM (1 mL) and added to PEG-Bisacid linker at 0 °C and stirred for 10 minutes at 0 °C under N<sub>2</sub>. In a separate flask, furan protected maleimide containing alcohol (164.1 mg, 0.736 mmol) and DMAP (8.2 mg, 0.067 mmol) were dissolved in anhydrous DCM (0.65 mL) and added to the activated PEG-Bisacid linker dropwise at room temperature. The reaction stirred at room temperature for 24 hours under N<sub>2</sub>. For the purification, solid N'-dicyclohexylurea residues were filtered and the reaction solvent was evaporated. The solid residue was precipitated in cold ether (50 mL x 3). The precipitate was dried under vacuum to yield pure product (480 mg, 72% yield, 90% coupling efficiency). <sup>1</sup>H NMR (CDCl<sub>3</sub>) δ (ppm): 6.51 (s, 4H), 5.26 (s, 4H), 4.23 (t, 4H), 4.07 (t, 4H), 3.85-3.35 (360H), 2.84 (s, 4H), 2.72 (t, 8H), 2.47 (m, 8H), 2.02 (m, 8H), 1.95 (m, 8H).

#### 3.4.4. Synthesis of PEG-Bismaleimide Crosslinker

The furan protected bismaleimide crosslinker (200 mg) is dried over 10 ml of toluene for three times and stayed on high vacuum for 24 hours until all the water residues were removed. The dried crosslinker is dissolved in dry toluene (90 mL) and r-DA reaction is run at 110 °C for 8 hours to obtain bismaleimide crosslinker as a pale yellow solid. <sup>1</sup>H NMR (CDCl<sub>3</sub>) δ (ppm): 6.71 (s, 1H), 4.23 (t, 1H), 4.07 (t, 1H), 3.85-3.35 (90H), 2.72 (t, 2H), 2.43 (m, 2H), 2.02 (m, 2H), 1.95 (m, 2H). (196 mg, 100% yield)

#### 3.5. Synthesis of Redox Responsive HA Hydrogels

Redox responsive HA-PEG hydrogels were synthesized by reacting HA-furan with disulfide bearing PEG-bismaleimide crosslinker dissolved separately in MES buffer (100 mM, pH 5.5). To inspect the effect of a difference in crosslinking density on hydrogel properties, three different sets of hydrogels with various crosslinking densities were investigated. On this basis, the molar ratios of furans on HA to maleimide groups on the crosslinker were calculated and hydrogels with 1/1, 1/0.75 and 1/0.5 furan to maleimide (F/M) molar ratios were synthesized. The concentration of HA-furan was constant at 1.15% w/v for each gel set where the concentration of the crosslinker varied from hydrogel to another. As an example, 8.7 mg of HA-furan with 57% DS (15 μmol of furan) was dissolved in 1 mL of MES buffer. The disulfide bearing PEG-bismaleimide crosslinker was used at concentrations as follows: 32.25 mg (15 μmol of maleimide, F/M=1:1), 24.19 mg (11.25 μmol of maleimide, F/M=1:0.75) and 16.125 mg (7.5 μmol of maleimide, F/M=1:0.5) were all dissolved in 290 μL of MES buffer. After the full dissolution of HA-furan and the bismaleimide crosslinker, the solutions were mixed and the samples were permitted to give gelation in bioshaker. (200 rpm) at 37 °C for 15h.

## 3.6. Characterization of Redox Responsive HA Hydrogels

### 3.6.1. Gelation Yields

The gelation yields of the HG1, HG2 and HG3 were individually calculated. Hydrogels were washed in dH<sub>2</sub>O to wash off the unreacted residues, freeze-dried and lyophilized to obtain dry gels. Weight of dry gels were divided by the weight sum of total polymer and crosslinker amount and this ratio was multiplied by 100 to calculate the percent yield of the gelation.

$$\text{Yield \%} = \frac{W_{\text{dry}}}{W_{\text{p+c}}} \times 100$$

### 3.6.2. Swelling Profiles

The water uptake capacities of hydrogels are measured by swelling tests. Hydrogel samples (10 mg, n=3) of HG1, HG2 and HG3 were lyophilized after multiple washes and dry hydrogels were put in 10 ml of dH<sub>2</sub>O at room temperature. At certain time points the hydrogels were removed out of water and weighed after the removal of excess water on gel surfaces.

### 3.6.3. SEM Images of the Microstructures

The microstructure and pore size of the hydrogels were investigated by Scanning Electron Microscope (SEM) accelerated at 10 kV. HG1, HG2 and HG3 were lyophilized, and then freeze-dried using liquid nitrogen. Freeze-dried samples were milled and cracked to obtain microsurfaces to capture images.

### **3.6.4. Rheological Studies**

The rheological properties of the hydrogels were followed by rheometer. 10 mg of hydrogel sample disks were allowed to swell in dH<sub>2</sub>O and their viscoelastic properties were investigated by frequency and amplitude sweep tests. The G' and G'' profiles of all hydrogels were observed for the angular frequency values scanned between 0.1 and 100 rad/s at 37 °C. The linear viscoelastic (LVE) region of the hydrogels were examined by amplitude sweep tests. The G' and G'' profiles of all hydrogels were observed for the angular frequency values scanned between 0.1 and 100% strain values at 37 °C at an angular frequency of 10 rad/s.

## **3.7. Degradation Studies**

### **3.7.1. Visual Degradation Studies**

For the visual examination of the degradation, FITC-BSA (1000 ppm) was physically encapsulated in two equivalent samples of 10 mg HG1 pre-gelation. Right after the gelation, gels were incubated in 5 mL of PBS only (pH=7.4) and 5 mL of DTT (5 mM) solutions. At 0 and 6th hours, gels were visualized under UV-light at  $\lambda=365$  nm.

### **3.7.2. Rheological Investigation of Stability in PBS**

10 mg of HG1, HG2 and HG3 were swollen in dH<sub>2</sub>O and time sweep test was run to observe the stability in PBS. For each gel, G' and G'' values of the hydrogels were recorded every minute at 37 °C in PBS buffer for 100 minutes and the G' values were recorded every

5 minutes continuously. Meanwhile, the angular frequency was kept at 10 rad/s in the pre-determined LVE region.

### **3.7.3. Rheological Investigation of Degradation in DTT**

10 mg of HG1, HG2 and HG3 were swollen in dH<sub>2</sub>O and time sweep test was run to observe the degradation rates. For each gel, G' and G'' values of the hydrogels were recorded every minute at 37 °C in presence of 10 mM of DTT in PBS buffer until the gel to sol transition where G'' crossovering the G' values was observed. Meanwhile, the angular frequency was kept at 10 rad/s in the pre-determined LVE region.

### **3.8. Encapsulation of FITC-BSA within the Hydrogels**

FITC-BSA was physically encapsulated in HG1 pre-gelation. 320 ppm of FITC-BSA (0.32 mg of FITC-BSA/ 1 ml of MES) solution in MES buffer (pH=5.5, 100 mM) was prepared. HG1 with radius and height of 50 mm (10 mg, yield=86%, n=9) was crosslinked in FITC-BSA dissolved in MES solution and FITC-BSA concentration was aimed to kept set in each gel.

### **3.9. Release of FIT-BSA from HG1 through Passive Diffusion and Redox Responsive Degradation**

To examine the passive diffusional and redox responsive release profiles of FITC-BSA from hydrogels, the following procedure was applied where the release medium was PBS for passive diffusion and 50 mM DTT to observe the redox responsive on-demand release. After the complete gelation, gels were first washed in 2 mL of dH<sub>2</sub>O with a duration 2 minutes to clear off and quantize the non-encapsulated FITC-BSA residues. (37 °C, 200

rpm) To investigate the passive release profiles, gels with radius and height of 50 mm (n=9) were incubated in wells of 24 well-plate where each containing 2 ml of the selected media (PBS, pH=7.4) Said plate was located in bioshaker (37 °C, 200 rpm) to initiate the release process. At pre-determined time points, 2 mL of medium was taken away from these vials and replaced with 2 ml of fresh medium. By the end of 72 h, PBS was removed and 2 mL of 50 mM DTT was added.

For the quantification of the cumulative release of FITC-BSA, the samples were analyzed with uv-spectrophotometer at 494 nm. The absorbance values were calculated as concentration using a calibration curve.

## 4. RESULTS AND DISCUSSION

### 4.1. Synthesis and Characterization of Furan Modified Hyaluronic Acid

The modification of HA was aimed to obtain gelation using Diels-Alder cycloaddition. Furan modified hyaluronic acid was synthesized by amidation reaction between the functionalizable carboxylic acid groups and furfuryl amine using 4-(4,6-dimethoxy-1,3,5-triazin-2-yl)-4-methylmorpholinium chloride (DMTMM) as a coupling agent (Figure 4.1). DMTMM is known as a high yielding agent activating the carboxylic acid groups on polysaccharide chains.[44] After the dialysis against ultrapure H<sub>2</sub>O the peaks of furan protons at 6.26, 6.36 and 7.45 ppm indicated the conjugation of furfuryl amine via the formation of an amide bond. The number of furan groups attached to HA are found to be 57%  $\pm$ 8, (n=9) by comparing the protons belonging the N-acetyl glucosamine group on the backbone with furan protons.

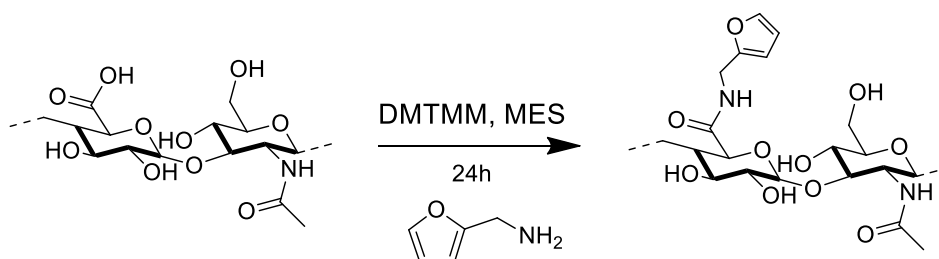


Figure 4.1. Synthesis of furan modified hyaluronic acid.

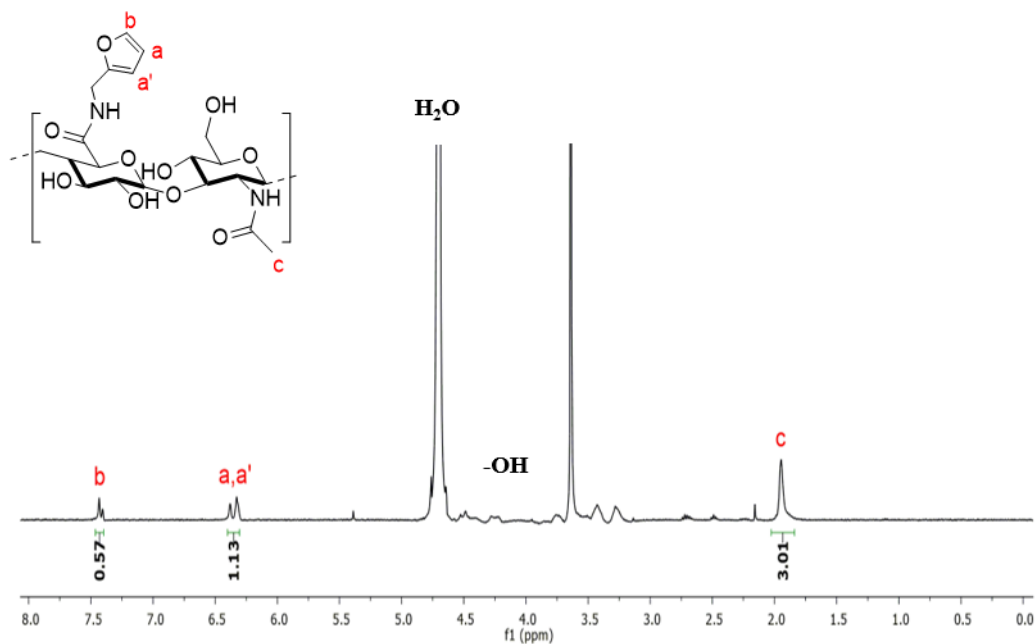


Figure 4.2.  $^1\text{H}$  NMR spectrum of the furan modified hyaluronic acid.

#### 4.2. Synthesis and Characterization of PEG-Bisacid

PEG-Bisacid was synthesized by coupling the 4 kDa PEG moieties with 4-4' dithiobutyric acid via DCC coupling where disulfide bearing carboxylic acid was activated to give esterification reaction with the alcohol groups at the end of the PEG chains. This path was particularly chosen to integrate the disulfide bonds in the crosslinker structure. In  $^1\text{H}$ NMR of the product, the triplet at 4.25 ppm belonged to the PEG protons adjacent to ester bond and the peaks at appearing 2.75, 2.5 and 2.05 ppm belonged to acid carbons and each individually standing for 8 protons. The peak at 2.75 was assigned to the protons of carbons adjacent to disulfide bonds since they were expected to be more deshielded due to sulfur atoms next to them where the peak at 2.05 ppm was assigned as the acid protons adjacent to the ester bond. The peak at 2.5 ppm was the protons belonging to acid carbon standing in between these other said two carbons, thus appeared as a multiplet. The broad peak appearing at 2.25 ppm is believed to belong to  $\text{H}_2\text{O}$ . When a drop of  $\text{D}_2\text{O}$  was added to the chloroform-

d in NMR tube, this peak almost disappeared and a new peak at 4.75 ppm appeared due to H-exchange.

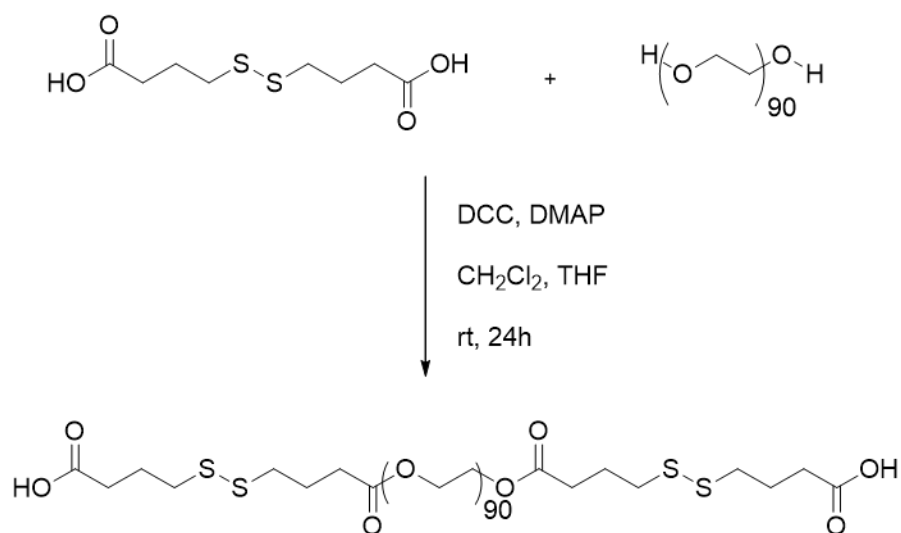


Figure 4.3. Synthesis of PEG-Bisacid.

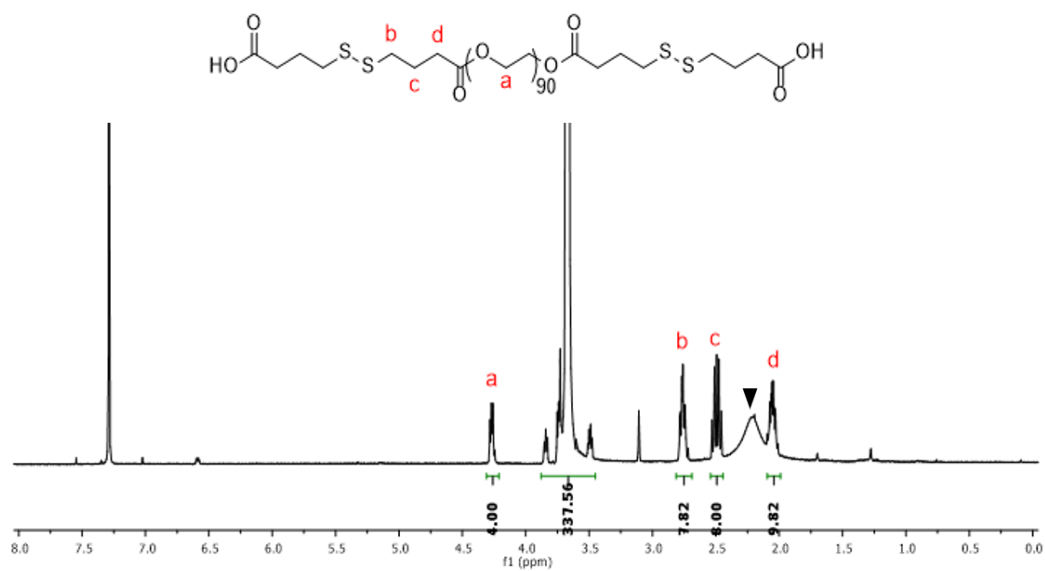


Figure 4.4. <sup>1</sup>H NMR spectra of PEG-Bisacid in CDCl<sub>3</sub>.

▼=water

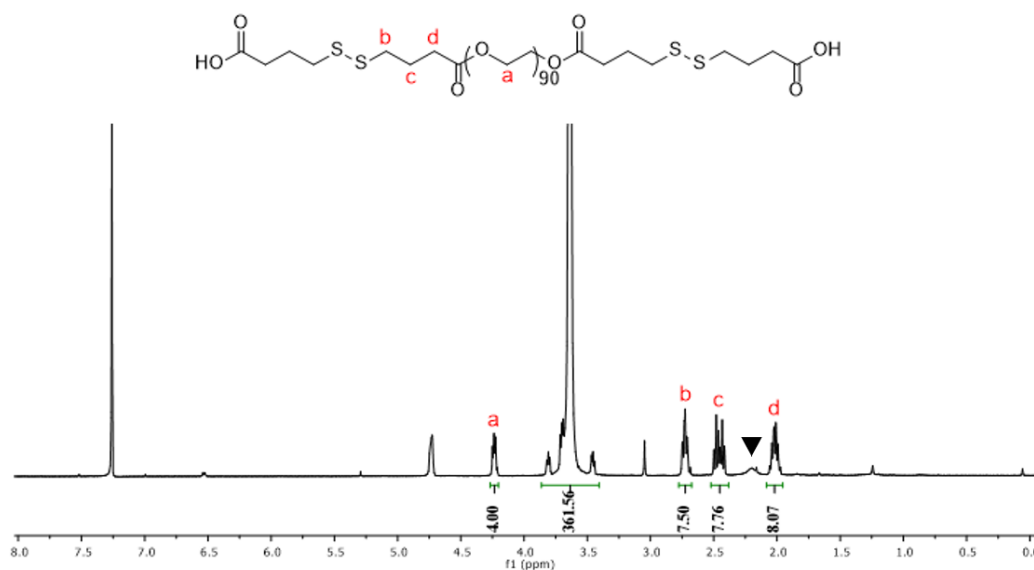


Figure 4.5.  $^1\text{H}$  NMR spectra of PEG-Bisacid in  $\text{CDCl}_3$  with  $\text{D}_2\text{O}$ .

▼=water

### 4.3. Synthesis and Characterization of Furan-Protected Bismaleimide Crosslinker

In order to obtain furan-protected PEG-bismaleimide, PEG-Bisacid was coupled with furan-protected maleimide containing alcohol to result in ester linkages in the presence of DCC and DMAP as coupling agents. PEG-Bisacid was dried azeotropically with toluene and then under high vacuum for 24 hours to remove any residual water that might affect the reaction yield. To understand the coupling efficiency of the reaction, the two proton peaks of furan at 5.25 and 6.5 ppm are integrated and compared with the peak at 4.25 which belongs to four of the PEG protons adjacent to the ester bonds. This ratio was expected to be one when the reaction worked with 100% efficiency. From the  $^1\text{H}$ NMR the highest conversion was found to be 90%. In general, the coupling efficiency of this reaction varied between 78-90% within different batches.

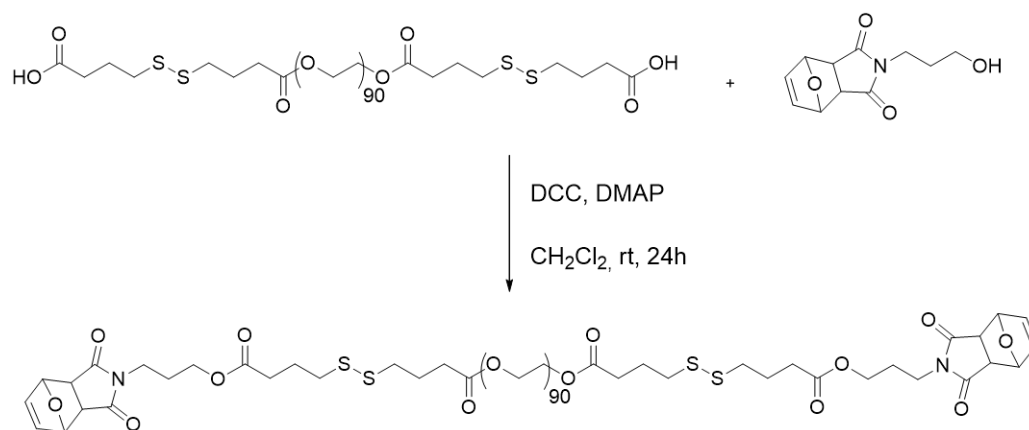
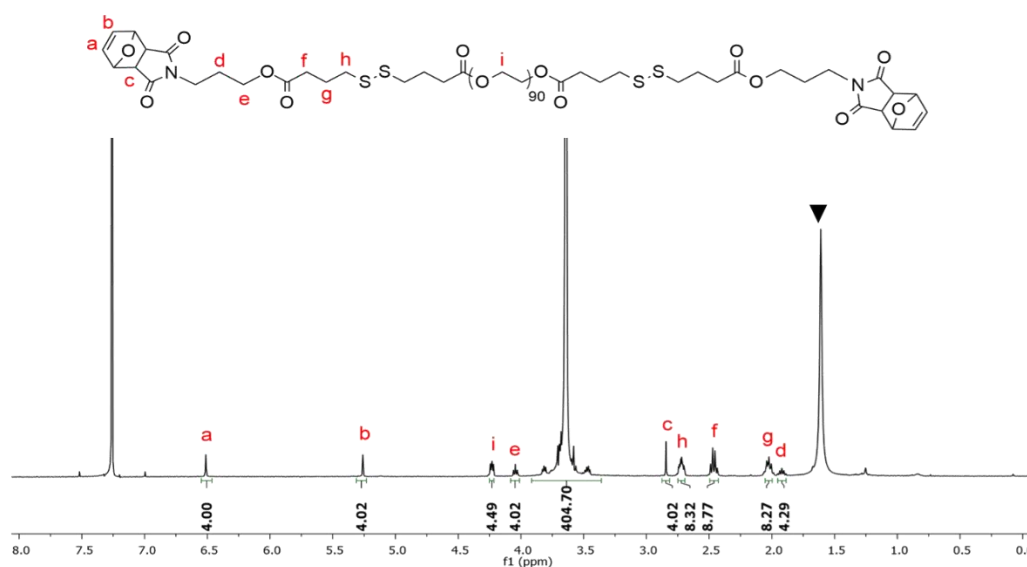


Figure 4.6. Synthesis of Furan Protected PEG-Bismaleimide.

Figure 4.7. <sup>1</sup>H NMR spectrum of Furan Protected PEG-Bismaleimide.

▼ = water

#### 4.4. Synthesis and Characterization of Bismaleimide Crosslinker

To achieve the crosslinker, furan-protected PEG-bismaleimides were transformed to PEG-maleimides by using retro Diels-Alder reaction (r-DA). Furan protected PEG-bismaleimide polymer was dried over toluene and under high vacuum to eliminate any

residual water. The product was dissolved in excess amount of anhydrous toluene and the reaction refluxed at 110 °C. After removal of toluene under reduced pressure, the desired product was obtained. In the HNMR spectrum of the product, the complete disappearance of the proton resonances from the bicyclic structure at 5.25 and 6.5 ppm and the appearance of a new singlet peak at 6.7 ppm which belongs to maleimide protons confirmed that the r-DA reaction was complete.

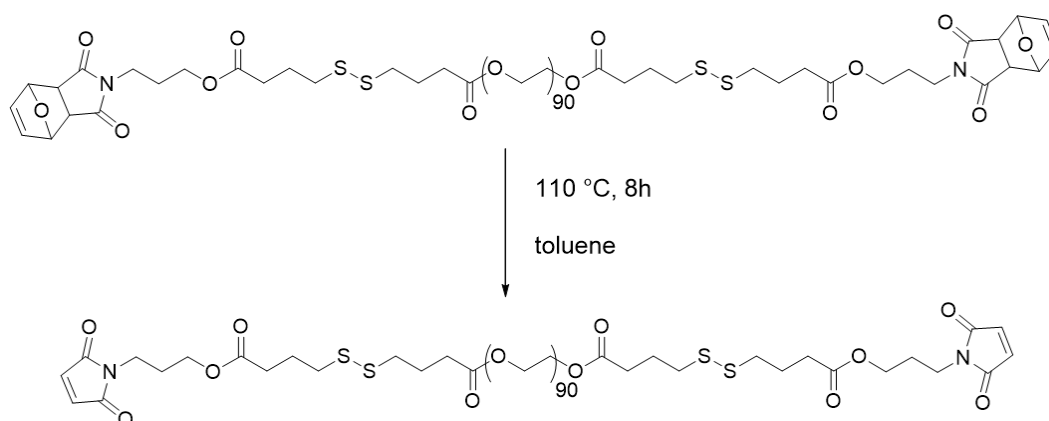


Figure 4.8. Synthesis of Bismaleimide Crosslinker.

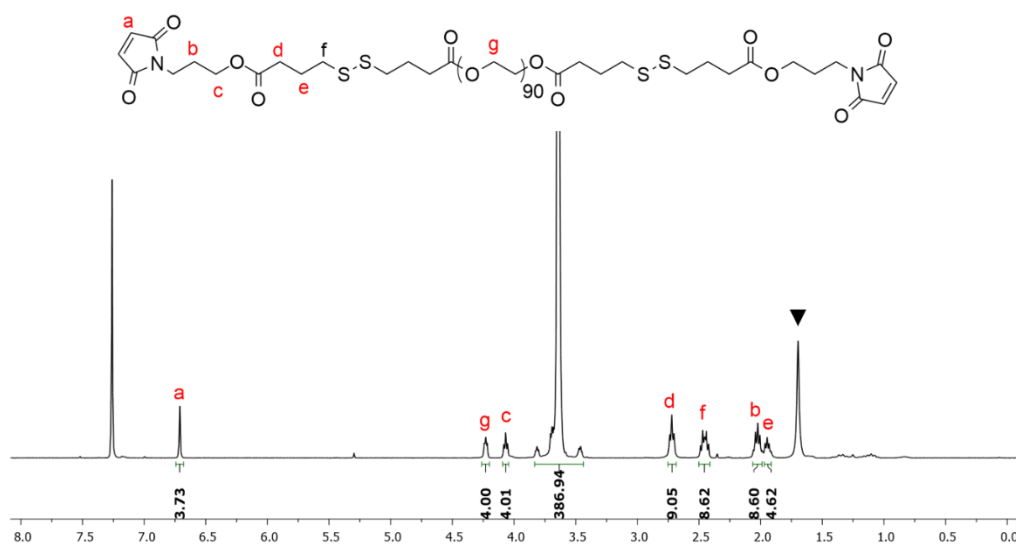


Figure 4.9. <sup>1</sup>H NMR spectrum of Bismaleimide Crosslinker.

▼ =water

#### 4.5. Synthesis and Characterization of Redox Responsive Hydrogels

The crosslinking of the redox responsive HA hydrogels were achieved using the Diels-Alder click reaction. (Figure 4.10) After the synthesis of bismaleimide crosslinker and the modification of HA with furan, said two groups are reaction to yield for a thermoset material in MES buffer (pH=5.5, 100 mM) as HA has enhanced solubility in acidic media. Notably, as DA is complete catalyst free click reaction these gels are expected not to contain any cytotoxic residues or by products after the removal of unreacted species by washings.

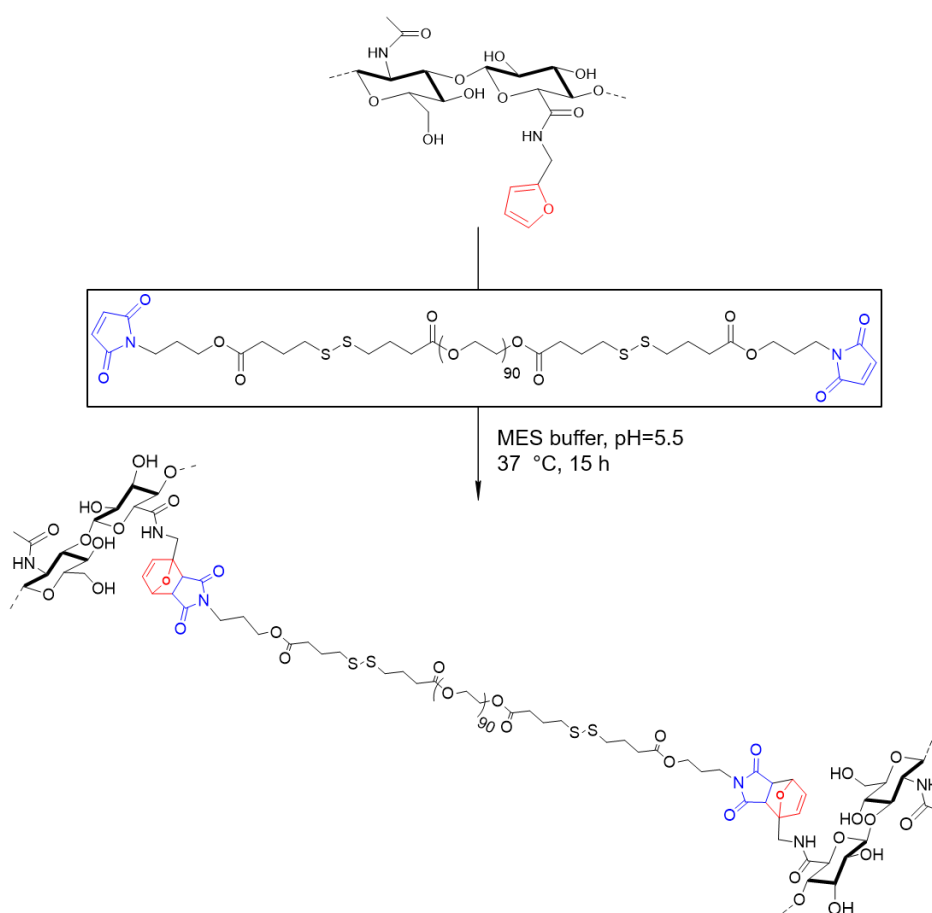


Figure 4.10. Synthesis of redox-responsive HA hydrogel.

Hydrogels with different F/M ratios, thus with different crosslinking densities were synthesized.

Table 4.1. Conversion of hydrogels with different crosslinking densities.

Hydrogel	Furan/Maleimide Ratio	Conversion
HG1	1/1	87 %
HG2	1/0.75	88 %
HG3	1/0.5	95 %

The end point detection of the hydrogel formation was assured by the inverted tube method where the gels exhibited a complete response against gravitational force. The hydrogels before the washings were transparent but yellowish due to a color from the crosslinker. Nevertheless, when the gels were washed and swelled significant amount of water, they turned to be colorless and fully transparent. (Figure 4.11) The obtained transparency carried importance in application of designed dressings as mentioned in ‘‘hydrogels as wound care materials’’ section.

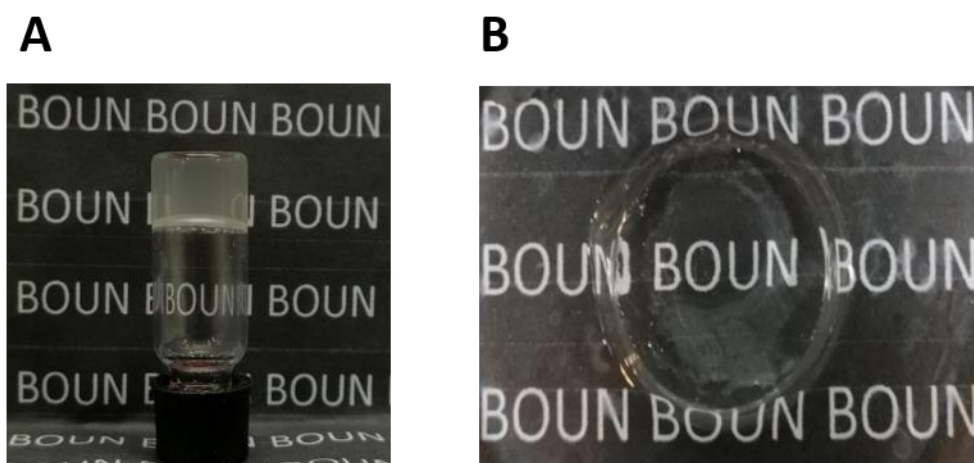


Figure 4.11. A) Inverted tube and B) swollen state images of HG1.

#### 4.6. Scanning Electron Microscope Images of Hydrogels

A variation in the amount of crosslinking is expected to cause a difference in the morphology and pores sizes of the hydrogels. To investigate their microstructures, lyophilized samples of hydrogels HG1, HG2 and HG3 were observed under SEM (Figure 4.12). Since these hydrogels were synthesized using furan modified HA, a functionalized NP with high molecular weights, the microstructures of the gels showed a porous but partly non-homogenous type microstructures.

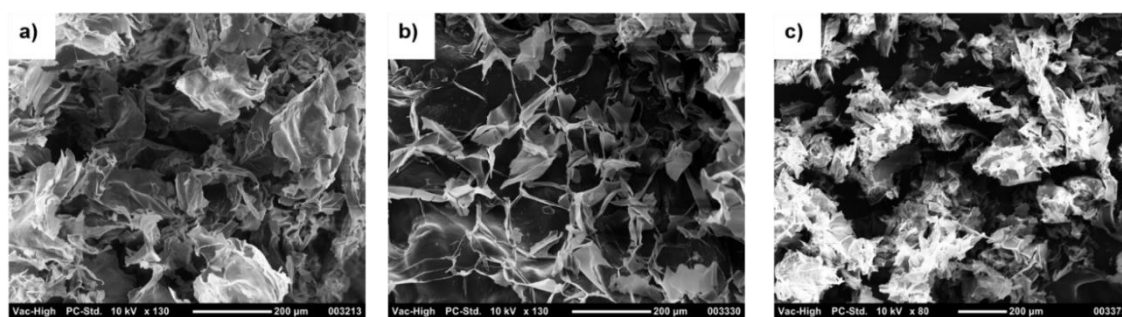


Figure 4.12. SEM images of a) HG1, b) HG2 and c) HG3. Scale bar: 200 µm.

#### 4.7. Swelling Profiles

The swelling abilities of HG1, HG2 and HG3 were studied. After 48 hours, hydrogels reached their equilibrium swelling points and according to the gravimetric calculations HG3 with the greatest pore size exhibited the highest swelling ratio as expected. However, in case of HG1 and HG2 this trend was opposite to expected porosity swelling relationship since HG1 (F/M=1:1) with more crosslinking density and smaller pore size showed a superior swelling ratio when compared to HG2 (F/M=1:0.75) (Figure 4.14) This unexpected profile is thought to be the result of another factor, which is the amount of PEG moieties within the gels which effects the swelling behaviour. Since HG1 and HG2 did not show a significant difference in their swelling profiles, the higher number of hydrophilic PEG moieties in HG1 is believed to result in a higher swelling ratio than HG2.

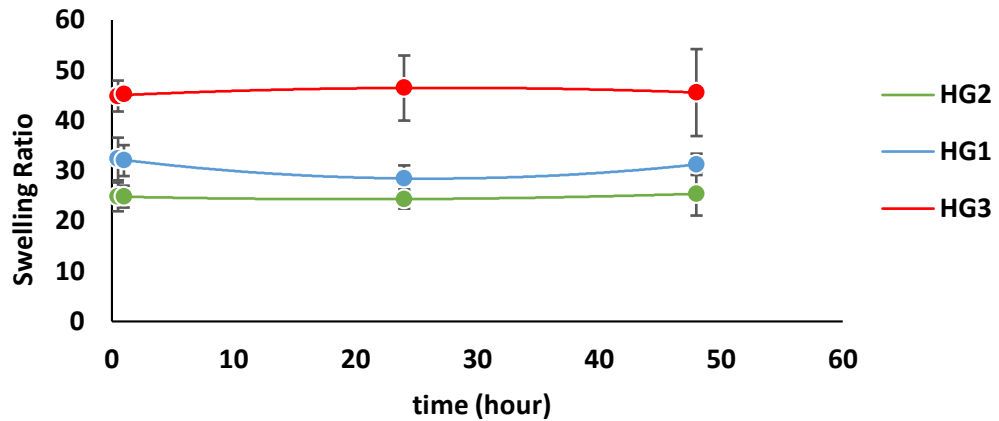


Figure 4.13. Swelling ratios of HG1, HG2 and HG3.

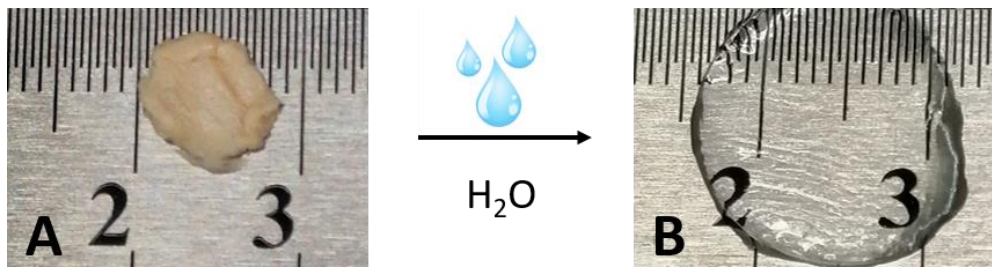


Figure 4.14. Visual images of HG3 in their A) dried and B) swollen states.

#### 4.8. Rheological Properties

The change in viscoelastic properties of the hydrogels according to the change in crosslinking density were investigated by using rheological analysis. To compare the differences of mechanical properties in hydrogels with varying crosslinking densities, frequency sweep and amplitude sweep tests were done. The frequency sweep tests were run to comprehend the time dependent behavior of the gels in terms of their storage modulus ( $G'$ ) abilities in a non-destructive deformation range. (0.1-100 rad/s)

In rheological analysis, the storage modulus ( $G'$ ) defines the ability of the hydrogel to store the deformation energy in a solid viscoelastic manner. Depending on this, with a

higher crosslinking density increased storage modulus values were expected. In addition, to be able to define the gel phase, a higher value of storage modulus in comparison to the loss modulus ( $G''$ ) is expected since  $G''$  stands for the modulus value of liquid state. As expected, HG1, HG2 and HG3 all individually demonstrated gel-like properties with  $G'$  values greater than their  $G''$  values. (Figures 4.15, 4.16 and 4.17) Another foreseen trend was that the hydrogels would show an increase in their  $G'$  values according to increased crosslinking densities which was also proved to exist. For HG1 the  $G'$  value was above  $10^3$  Pa whereas for HG2 and HG3 this value was under  $10^3$  Pa. (Figure 4.18)

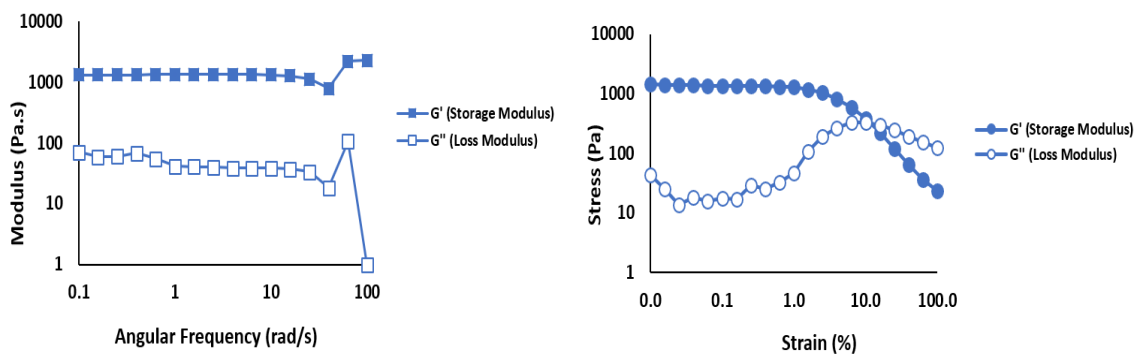


Figure 4.15. Frequency Sweep (Right) and Amplitude Sweep (Left) tests of HG1.

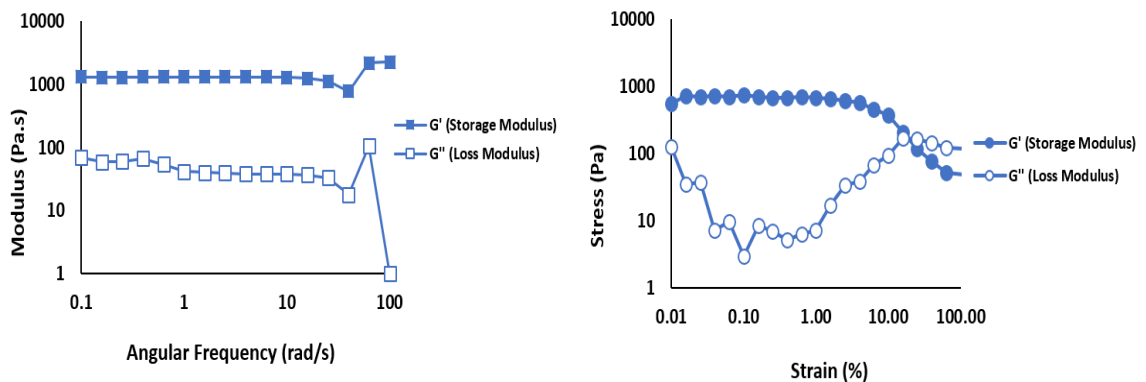


Figure 4.16. Frequency Sweep (left) and Amplitude Sweep (right) tests of HG2.

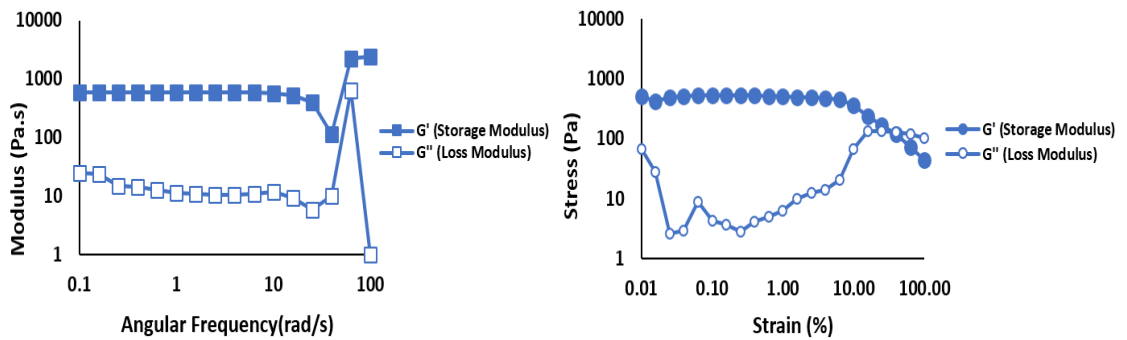


Figure 4.17. Frequency Sweep (left) and Amplitude Sweep (right) tests of HG3.

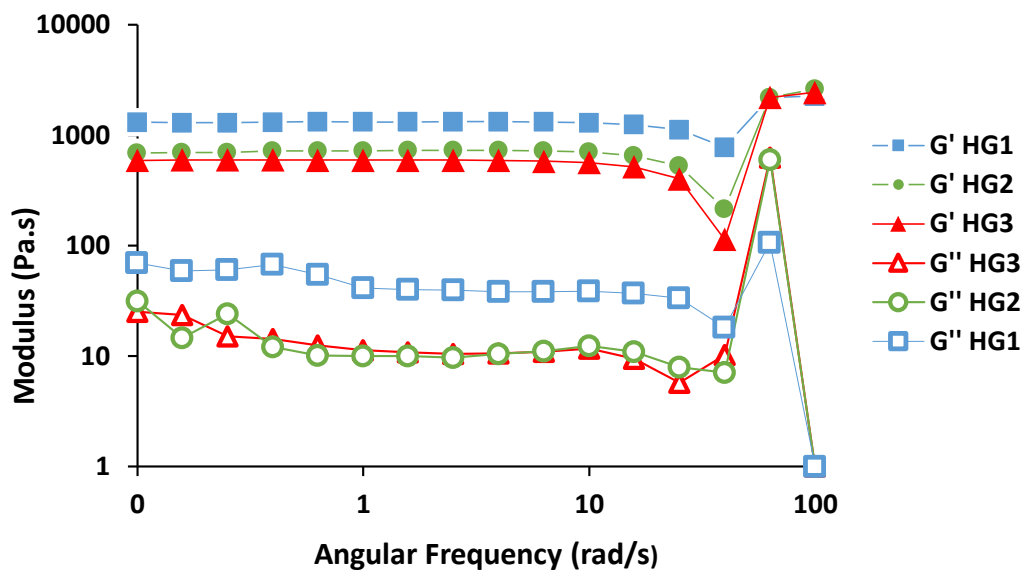


Figure 4.18. Combined Frequency Sweep Tests of HG1, HG2 and HG3.

#### 4.9. Degradation Profiles

Since this hydrogel system is aimed as an on-demand degradable wound dressing, the redox-responsive degradation profiles and the change in profiles upon an alteration in crosslinking density are investigated. To perform the desired on demand removal of the biomaterial during or after the treatment, these dressing were expected to be stable in PBS

but also demonstrate the full dissolution in a reducing environment. To achieve the on demand degradation property, redox responsive disulfide bonds were integrated within the crosslinker structure. The degradation profiles of HG1 was observed by visual degradation test where degradation profiles HG1, HG2 and HG3 were all investigated with rheological tests.

For the examination of visual degradation, FITC-BSA was encapsulated within the HG1 during the gelation and the degradation in presence of 5 mM DTT was followed under UV light (Figure 4.20). To prove that DTT was the only parameter which caused the degradation, HG1 was also treated only with PBS as a control experiment. By the end of 6 hours at rt, DTT dependent degradation of HG1 was observed as the FITC-BSA was fully dispersed in the solution without any hydrogel leftover (Figure 4.21). However, HG1 treated with PBS only did not degrade and only a lower intensity fluorescence of FITC was observed as a result of released FITC-BSA through passive diffusion (Figure 4.20).

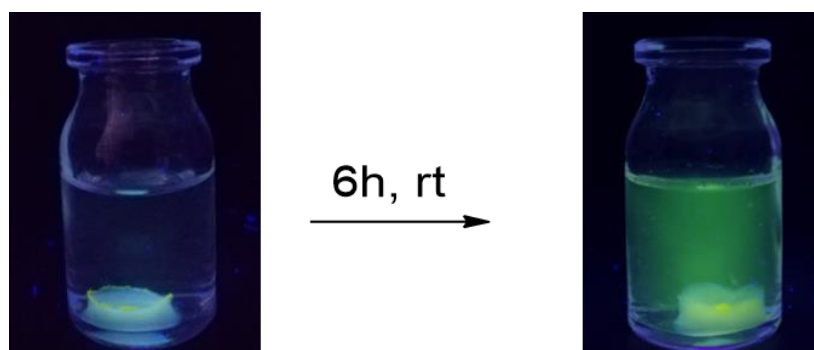


Figure 4.19. Visual stability of FITC encapsulated HG1 encapsulates images in only PBS at rt.

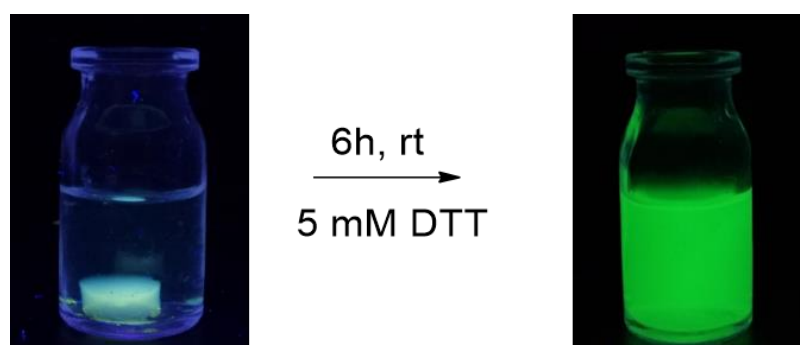


Figure 4.20. Visual degradation of HG1 in 5 mM DTT at rt.

The sol-gel transition term stands to define the crossover point of  $G'$  and  $G''$  values of a liquid during the gelation process. The domination of  $G'$  over  $G''$  is accepted as an indication of the material showing gel-like behaviour rather than its liquid state properties. The reverse of the sol-gel transition suggests the inversed process, that is gel to sol transition, where  $G''$  crosses over  $G'$  and the viscoelastic properties of the material are lost due to a domination of liquid behaviour. Using this information, time dependent redox responsive degradation profiles of the hydrogels were inspected via time sweep tests. HG1, HG2 and HG3 were all allowed to stay in PBS (pH=7.4) to certain swelling points. To prove the stability of HG1, HG2 and HG3 in PBS at 37 °C time sweep test was performed first in only PBS for 100 minutes. (Figure 4.21) Following this, the gels were treated with disulfide reducing agent DTT (10 mM) and the gel to sol transition points with respect to time were followed as a function of time. As expected, HG1 with the highest crosslinking density, thus involving the highest number of disulfide bonds displayed the longest interval of degradation with an approximate of 210 minutes (Figure 4.22) whereas HG2 and HG3 degraded approximately in 110 (Figure 4.23) and 97 (Figure 4.24) minutes, respectively. This trend proved that these redox responsive HA-hydrogels exhibited tunable redox responsive degradation profiles adjusting the disulfide bearing crosslinking density.

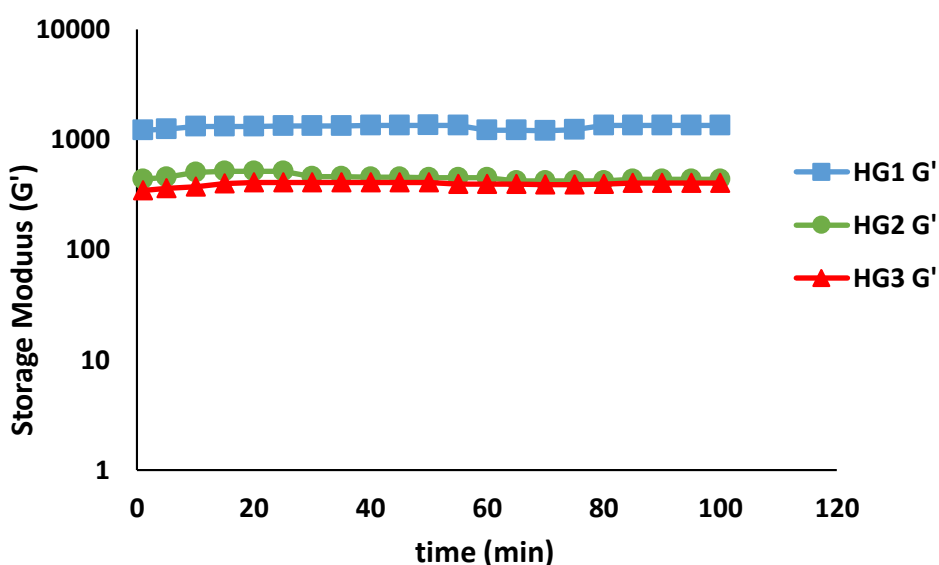


Figure 4.21. Stability of HG1, HG2, and HG3 in PBS.

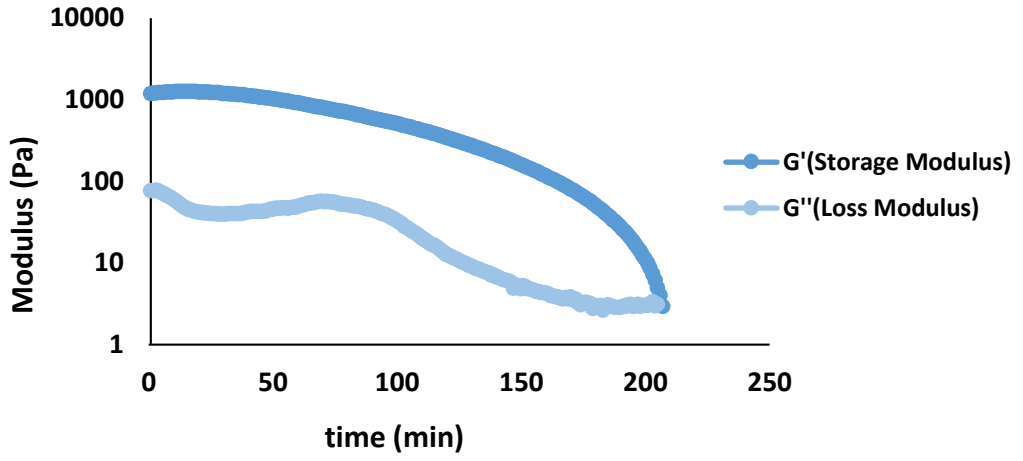


Figure 4.22. Time Sweep Test of HG1 in 10 mM DTT.

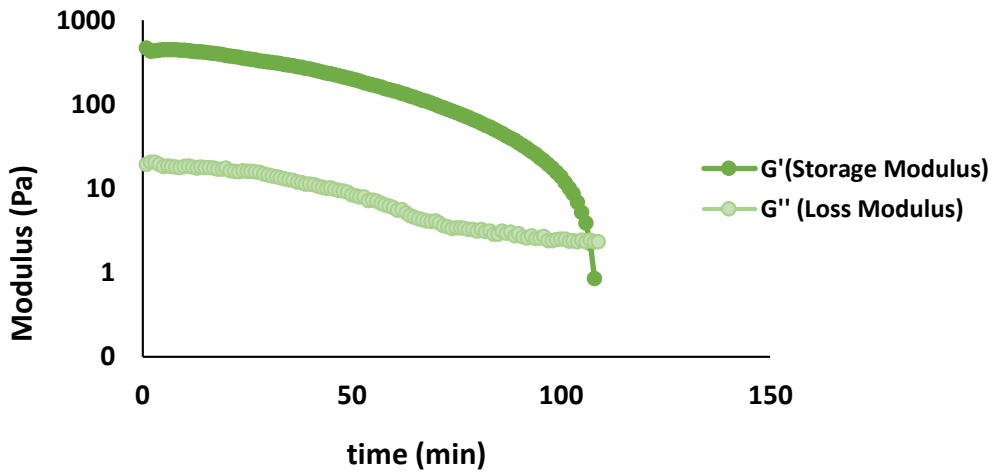


Figure 4.23. Time Sweep Test of HG2 in 10 mM DTT.

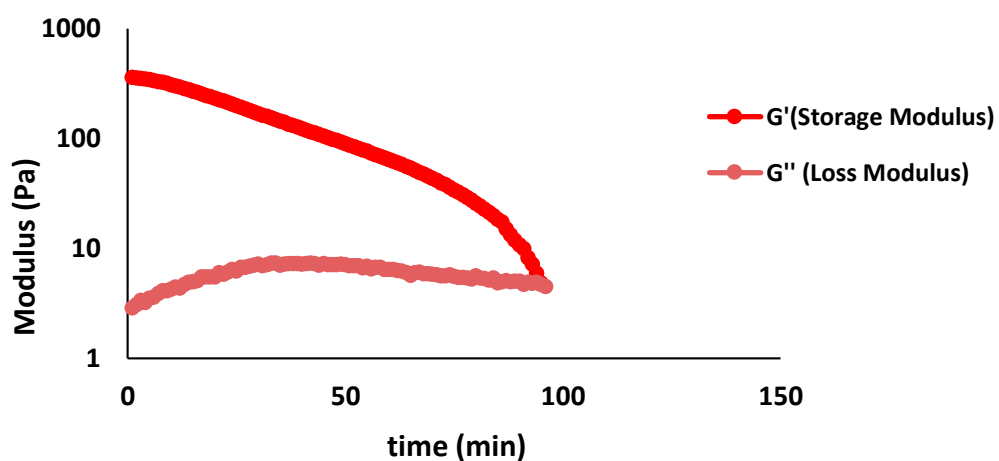


Figure 4.24. Time Sweep Test of HG3 in 10 mM DTT.

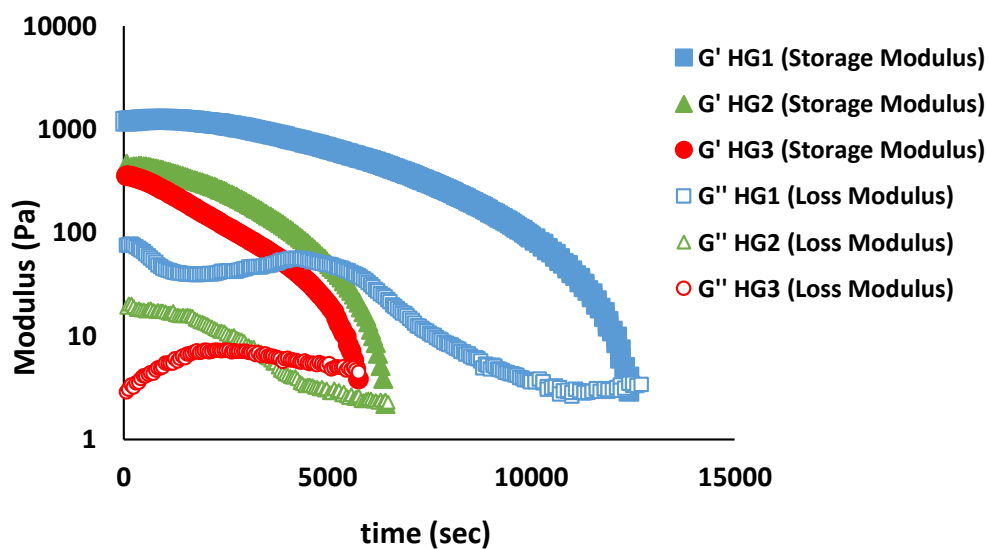


Figure 4.25. Redox responsive degradation of HG1, HG2 and HG3 in rheometer as a function of time.

#### **4.10. Diffusional and On-Demand Release Profiles of FITC-BSA from HG1**

The local delivery of a protein was aimed since this hydrogel system was designed to carry the potential of a local delivery material of tissue regenerative proteins. For this purpose, BSA was chosen as a model protein and the diffusional and on-demand release profiles of HG1 were investigated. To determine the BSA concentration using UV-spectroscopy, FITC conjugated BSA was used. First, hydrogels were let to perform the passive release of BSA in PBS (1x, pH=7.4) only. It was observed that hydrogels released 36% of encapsulated FITC-BSA by the end of 6 h and at 72<sup>nd</sup> h 55% of the total FITC-BSA was released from the gels. At 72<sup>nd</sup> hour, 50 mM of DTT was added to the media to investigate the on demand release of HG1 due to redox responsive degradation. A rapid change at the amount of BSA release was anticipated since the gels were designed to degrade completely in presence of DTT. As expected, upon the addition of 50 mM DTT the gels degraded rapidly and a total of 30% of the encapsulated BSA was released from HG1. The release study showed the successful sustained and on-demand release abilities of HG1 which acted as a cargo system for BSA protein. Importantly, it was also seen that HG1 was also able to deliver a total of 85% of the protein cargo upon on-degradation. Large deviations were observed at 4<sup>th</sup> and 5<sup>th</sup> hours.

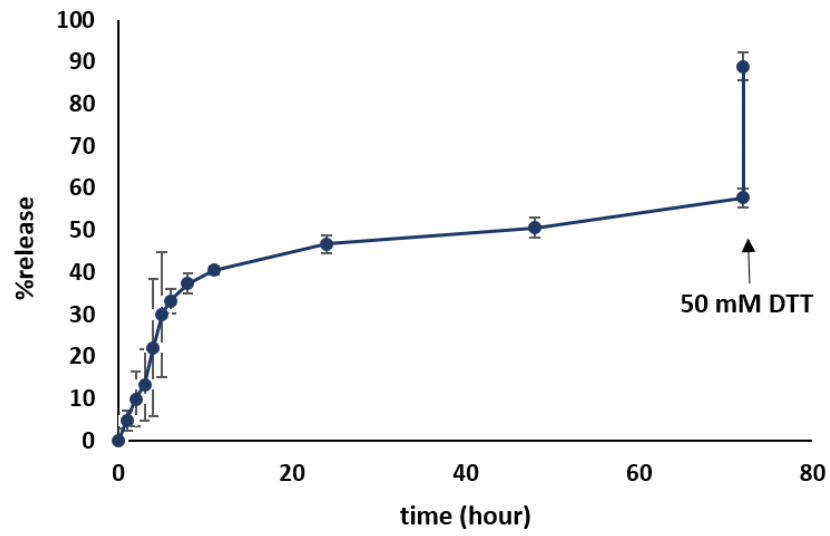


Figure 4.26. Release of FITC-BSA from HG1 in PBS and upon the addition of 50 mM DTT.

## 5. CONCLUSIONS

In this thesis, hyaluronic acid based redox-responsive hydrogels were synthesized using Diels-Alder click reaction to be used for wound care applications, explicitly to apply as dressings for burn wounds. For this purpose, the carboxylic acid groups on HA (200 kDa) were modified with furan groups and a PEG (4kDa) moieties and disulfide bonds bearing bismaleimide crosslinker was also synthesized. Furan groups on HA further gave DA reactions with maleimides of the crosslinker to result in hydrogel formation. Hydrogels with different crosslinking ratios were synthesized to understand the effect of crosslinking density on mechanical properties. It was observed these hydrogels exhibited higher storage modulus values with increased crosslinking density. SEM images of hydrogels with different crosslinking densities showed an increase in porosity with a decrease in crosslinking density, as expected. Coherently, in presence of DTT (10 mM) hydrogels with less crosslinking density thus with a lower number of disulfide bonds and bigger pore size degraded more rapidly according to the rheological analysis. The release profiles of physically encapsulated FITC-BSA in the hydrogel with highest crosslinking density were studied in PBS and upon the addition of 50 mM DTT. Both sustained and on-demand delivery of the selected macromolecular cargo, FITC-BSA through the gels were observed. As a result, these hydrogels are highly biocompatible and promising materials with tunable degradation features and local protein delivery abilities which can be used as dressings during the wound care process. However, the bio applicability and efficacy of these gels still needs to be further investigated through in vitro and in vivo studies.

## REFERENCES

1. Vega, S.L., M.Y. Kwon, and J.A. Burdick, "Recent Advances In Hydrogels For Cartilage Tissue Engineering.", *European Cells and Materials*, Vol. 33, pp. 59–75, 2017.
2. Li, J., and D.J. Mooney, "Designing Hydrogels For Controlled Drug Delivery.", *Nature Reviews Materials*, Vol. 1 2016.
3. Klouda, L., "Thermoresponsive Hydrogels In Biomedical Applications A Seven-Year Update.", *European Journal of Pharmaceutics and Biopharmaceutics*, Vol. 97, pp. 338–349, 2015.
4. Tomatsu, I., K. Peng, and A. Kros, "Photoresponsive Hydrogels For Biomedical Applications.", *Advanced Drug Delivery Reviews*, Vol. 63, pp. 1257–1266, 2011.
5. Erol, O., A. Pantula, W. Liu, and D.H. Gracias, "Transformer Hydrogels: A Review.", *Advanced Materials Technologies*, Vol. 4, pp. 1–27, 2019.
6. Teßmar, J., F. Brandl, and A. Göpferich, "Hydrogels For Tissue Engineering.", *Fundamentals of Tissue Engineering and Regenerative Medicine*, Vol. 101, pp. 495–517, 2009.
7. Caló, E., and V. V. Khutoryanskiy, "Biomedical Applications Of Hydrogels: A Review Of Patents And Commercial Products.", *European Polymer Journal*, Vol. 65, pp. 252–267, 2015.
8. Hoare, T.R., and D.S. Kohane, "Hydrogels In Drug Delivery: Progress And Challenges.", *Polymer*, Vol. 49, pp. 1993–2007, 2008.
9. Mathur, A.M., S.K. Moorjani, B. Scranton, and E. Lansing, "Journal Of Macromolecular Science , Part C Methods For Synthesis Of Hydrogel Networks : A Review.", *Journal of Macromolecular Science*, Vol. C36, pp. 37–41, 2006.
10. Knop, K., R. Hoogenboom, D. Fischer, and U.S. Schubert, "Poly(Ethylene Glycol) In Drug Delivery: Pros And Cons As Well As Potential Alternatives.", *Angewandte Chemie - International Edition*, Vol. 49, pp. 6288–6308, 2010.
11. Prestwich, G.D., D.M. Marecak, J.F. Marecek, K.P. Vercruyssen, and M.R. Ziebell, "Controlled Chemical Modification Of Hyaluronic Acid: Synthesis, Applications, And Biodegradation Of Hydrazide Derivatives.", *Journal of Controlled Release*, Vol. 53, pp. 93–103, 1998.
12. Feksa, L.R., E.A. Troian, C.D. Muller, F. Viegas, A.B. Machado, and V.C. Rech, "Hydrogels For Biomedical Applications.", *Nanostructures for the Engineering of*

- Cells, Tissues and Organs: From Design to Applications*, Vol. 64, pp. 403–438, 2018.
13. Singh, M.R., S. Patel, and D. Singh, “Natural Polymer-Based Hydrogels as Scaffolds for Tissue Engineering.”, *Nanobiomaterials in Soft Tissue Engineering: Applications of Nanobiomaterials* 2016.
  14. Cristina, A., and D.O. Gonzalez, “Abd-91-05-0614.”, *Anais Brasileiros de Dermatologia*, pp. 614–620, 2016.
  15. Martin, C., W.L. Low, M.C.I.M. Amin, I. Radecka, P. Raj, and K. Kenward, “Current Trends In The Development Of Wound Dressings, Biomaterials And Devices.”, *Pharmaceutical Patent Analyst*, Vol. 2, pp. 341–359, 2013.
  16. J, W., C. H, C. F, and S. A, “Dressings For Treating Superficial And Partial Thickness Burns.”, *Cochrane* 2013.
  17. Madaghiele, M., A. Sannino, L. Ambrosio, and C. Demitri, “Polymeric Hydrogels For Burn Wound Care: Advanced Skin Wound Dressings And Regenerative Templates.”, *Burns & Trauma*, Vol. 2, pp. 153, 2014.
  18. Rippon, M., P. Davies, and R. White, “Taking The Trauma Out Of Wound Care: The Importance Of Undisturbed Healing.”, *Journal of Wound Care*, Vol. 21, pp. 359–368, 2012.
  19. Chen, M., J. Tian, Y. Liu, H. Cao, R. Li, J. Wang, J. Wu, and Q. Zhang, “Dynamic Covalent Constructed Self-Healing Hydrogel For Sequential Delivery Of Antibacterial Agent And Growth Factor In Wound Healing.”, *Chemical Engineering Journal*, Vol. 373, pp. 413–424, 2019.
  20. Kirker, K.R., Y. Luo, J.H. Nielson, J. Shelby, and G.D. Prestwich, “Glycosaminoglycan Hydrogel Films As Bio-Interactive Dressings For Wound Healing.”, *Biomaterials*, Vol. 23, pp. 3661–3671, 2002.
  21. Lu, H., L. Yuan, X. Yu, C. Wu, D. He, and J. Deng, “Recent Advances Of On-Demand Dissolution Of Hydrogel Dressings.”, *Burns & Trauma*, Vol. 6, pp. 1–13, 2018.
  22. Putzu, M., F. Gräter, M. Elstner, and T. Kubař, “On The Mechanism Of Spontaneous Thiol-Disulfide Exchange In Proteins.”, *Physical Chemistry Chemical Physics*, Vol. 20, pp. 16222–16230, 2018.
  23. Yi, M.C., and C. Khosla, “Thiol–Disulfide Exchange Reactions In The Mammalian Extracellular Environment.”, *Annual Review of Chemical and Biomolecular Engineering*, Vol. 7, pp. 197–222, 2016.
  24. Altinbasak, I., R. Sanyal, and A. Sanyal, “Best Of Both Worlds: Diels-Alder Chemistry

- Towards Fabrication Of Redox-Responsive Degradable Hydrogels For Protein Release.”, *RSC Advances*, Vol. 6, pp. 74757–74764, 2016.
25. Yue, B., “Biology Of The Extracellular Matrix: An Overview.”, *Journal of Glaucoma*, Vol. 23, pp. S20–S23, 2014.
  26. Burdick, J.A., and G.D. Prestwich, “Hyaluronic Acid Hydrogels For Biomedical Applications.”, *Advanced Materials*, Vol. 23, pp. 41–56, 2011.
  27. Termeer, C., J.P. Sleeman, and J.C. Simon, “Hyaluronan - Magic Glue For The Regulation Of The Immune Response?”, *Trends in Immunology*, Vol. 24, pp. 112–114, 2003.
  28. Burdick, J.A., C. Chung, X. Jia, M.A. Randolph, and R. Langer, “Controlled Degradation And Mechanical Behavior Of Photopolymerized Hyaluronic Acid Networks.”, *Biomacromolecules*, Vol. 6, pp. 386–391, 2005.
  29. Kim, H., H. Jeong, S. Han, S. Beack, B.W. Hwang, M. Shin, S.S. Oh, and S.K. Hahn, “Hyaluronate And Its Derivatives For Customized Biomedical Applications.”, *Biomaterials*, Vol. 123, pp. 155–171, 2017.
  30. Necas, J., L. Bartosikova, P. Brauner, and J. Kolar, “Hyaluronic Acid (Hyaluronan): A Review.”, *Veterinarni Medicina*, Vol. 53, pp. 397–411, 2008.
  31. Luan, S., Y. Zhu, X. Wu, Y. Wang, F. Liang, and S. Song, “Hyaluronic-Acid-Based PH-Sensitive Nanogels for Tumor-Targeted Drug Delivery.”, *ACS Biomaterials Science and Engineering*, Vol. 3 2017.
  32. Chiesa, E., R. Dorati, B. Conti, T. Modena, E. Cova, F. Meloni, and I. Genta, “Hyaluronic Acid-Decorated Chitosan Nanoparticles For CD44-Targeted Delivery Of Everolimus.”, *International Journal of Molecular Sciences*, Vol. 19 2018.
  33. Prestwich, G.D., “Hyaluronic Acid-Based Clinical Biomaterials Derived For Cell And Molecule Delivery In Regenerative Medicine.”, *Journal of Controlled Release*, Vol. 155, pp. 193–199, 2011.
  34. Manzi, G., N. Zoratto, S. Matano, R. Sabia, C. Villani, T. Coviello, P. Matricardi, and C. Di Meo, “‘Click’ Hyaluronan Based Nanohydrogels As Multifunctionalizable Carriers For Hydrophobic Drugs.”, *Carbohydrate Polymers*, Vol. 174, pp. 706–715, 2017.
  35. Yang, J., Y.S. Zhang, K. Yue, and A. Khademhosseini, “Cell-Laden Hydrogels For Osteochondral And Cartilage Tissue Engineering.”, *Acta Biomaterialia*, Vol. 57, pp. 1–25, 2017.

36. Gupta, D., C.H. Tator, and M.S. Shoichet, “Fast-Gelling Injectable Blend Of Hyaluronan And Methylcellulose For Intrathecal, Localized Delivery To The Injured Spinal Cord.”, *Biomaterials*, Vol. 27, pp. 2370–2379, 2006.
37. Kim, J., I.S. Kim, T.H. Cho, K.B. Lee, S.J. Hwang, G. Tae, I. Noh, S.H. Lee, Y. Park, and K. Sun, “Bone Regeneration Using Hyaluronic Acid-Based Hydrogel With Bone Morphogenic Protein-2 And Human Mesenchymal Stem Cells.”, *Biomaterials*, Vol. 28, pp. 1830–1837, 2007.
38. Wang, X., J. He, Y. Wang, and F.Z. Cui, “Hyaluronic Acid-Based Scaffold For Central Neural Tissue Engineering.”, *Interface Focus*, Vol. 2, pp. 278–291, 2012.
39. Shu, X.Z., Y. Liu, F. Palumbo, and G.D. Prestwich, “Disulfide-Crosslinked Hyaluronan-Gelatin Hydrogel Films: A Covalent Mimic Of The Extracellular Matrix For In Vitro Cell Growth.”, *Biomaterials*, Vol. 24, pp. 3825–3834, 2003.
40. Crescenzi, V., L. Cornelio, C. Di Meo, S. Nardecchia, and R. Lamanna, “Novel Hydrogels Via Click Chemistry: Synthesis And Potential Biomedical Applications.”, *Biomacromolecules*, Vol. 8, pp. 1844–1850, 2007.
41. Bhakta, G., B. Rai, Z.X.H. Lim, J.H. Hui, G.S. Stein, A.J. van Wijnen, V. Nurcombe, G.D. Prestwich, and S.M. Cool, “Hyaluronic Acid-Based Hydrogels Functionalized With Heparin That Support Controlled Release Of Bioactive BMP-2.”, *Biomaterials*, Vol. 33, pp. 6113–6122, 2012.
42. Leach, J.B., and C.E. Schmidt, “Characterization Of Protein Release From Photocrosslinkable Hyaluronic Acid-Polyethylene Glycol Hydrogel Tissue Engineering Scaffolds.”, *Biomaterials*, Vol. 26, pp. 125–135, 2005.
43. Ibrahim, S., C.R. Kothapalli, Q.K. Kang, and A. Ramamurthi, “Characterization Of Glycidyl Methacrylate - Crosslinked Hyaluronan Hydrogel Scaffolds Incorporating Elastogenic Hyaluronan Oligomers.”, *Acta Biomaterialia*, Vol. 7, pp. 653–665, 2011.
44. Nimmo, C.M., S.C. Owen, and M.S. Shoichet, “Diels-Alder Click Cross-Linked Hyaluronic Acid Hydrogels For Tissue Engineering.”, *Biomacromolecules*, Vol. 12, pp. 824–830, 2011.
45. Smith, L.J., S.M. Taimoory, R.Y. Tam, A.E.G. Baker, N. Bintah Mohammad, J.F. Trant, and M.S. Shoichet, “Diels-Alder Click-Cross-Linked Hydrogels With Increased Reactivity Enable 3D Cell Encapsulation.”, *Biomacromolecules*, Vol. 19, pp. 926–935, 2018.
46. Kolb, H.C., M.G. Finn, and K.B. Sharpless, “Click Chemistry: Diverse Chemical

- Function From A Few Good Reactions.”, *Angewandte Chemie - International Edition*, Vol. 40, pp. 2004–2021, 2001.
47. McKay, C.S., and M.G. Finn, “Click Chemistry In Complex Mixtures: Bioorthogonal Bioconjugation.”, *Chemistry and Biology*, Vol. 21, pp. 1075–1101, 2014.
48. Hein, C.D., X.M. Liu, and D. Wang, “Click Chemistry, A Powerful Tool For Pharmaceutical Sciences.”, *Pharmaceutical Research*, Vol. 25, pp. 2216–2230, 2008.
49. Mou, X.Z., X.Y. Chen, J. Wang, Z. Zhang, Y. Yang, Z.X. Shou, Y.X. Tu, X. Du, C. Wu, Y. Zhao, L. Qiu, P. Jiang, C. Chen, D.S. Huang, and Y.Q. Li, “Bacteria-Instructed Click Chemistry Between Functionalized Gold Nanoparticles For Point-Of-Care Microbial Detection.”, *ACS Applied Materials and Interfaces*, Vol. 11, pp. 23093–23101, 2019.
50. Mardpour, S., M.H. Ghanian, H. Sadeghi-Abandansari, Saeid Mardpour, A. Nazari, F. Shekari, and H. Baharvand, “Hydrogel-Mediated Sustained Systemic Delivery Of Mesenchymal Stem Cell-Derived Extracellular Vesicles Improves Hepatic Regeneration In Chronic Liver Failure.”, *ACS Applied Materials and Interfaces*, Vol. 11, pp. 37421–37433, 2019.
51. Seo, J., S.H. Park, M.J. Kim, H.J. Ju, X.Y. Yin, B.H. Min, and M.S. Kim, “Injectable Click-Crosslinked Hyaluronic Acid Depot To Prolong Therapeutic Activity In Articular Joints Affected By Rheumatoid Arthritis.”, *ACS Applied Materials and Interfaces*, Vol. 11, pp. 24984–24998, 2019.
52. Si, H., T. Xing, Y. Ding, H. Zhang, R. Yin, and W. Zhang, “3D Bioprinting Of The Sustained Drug Release Wound Dressing With Double-Crosslinked Hyaluronic-Acid-Based Hydrogels.”, *Polymers*, Vol. 11 2019.
53. Gandini, A., “The Furan/Maleimide Diels-Alder Reaction: A Versatile Click-Unclick Tool In Macromolecular Synthesis.”, *Progress in Polymer Science*, Vol. 38, pp. 1–29, 2013.
54. Or, T.H.E.R.D., and R. Reaction, “<retroDA.Pdf>.”, Vol. 4389 1967.
55. Oz, Y., and A. Sanyal, “The Taming Of The Maleimide: Fabrication Of Maleimide-Containing ‘Clickable’ Polymeric Materials.”, *Chemical Record*, Vol. 18, pp. 570–586, 2018.
56. Yu, F., X. Cao, Y. Li, and X. Chen, “Diels-Alder Click-Based Hydrogels For Direct Spatiotemporal Postpatterning Via Photoclick Chemistry.”, *ACS Macro Letters*, Vol. 4, pp. 289–292, 2015.
57. Hu, X., Z. Gao, H. Tan, H. Wang, X. Mao, and J. Pang, “An Injectable Hyaluronic Acid-

- Based Composite Hydrogel By DA Click Chemistry With PH Sensitive Nanoparticle For Biomedical Application.”, *Frontiers in Chemistry*, Vol. 7, pp. 1–11, 2019.
58. Neubert, B.J., and B.B. Snider, “Synthesis Of ( $\pm$ )-Phloeodictine A1.”, *Organic Letters*, Vol. 5, pp. 765–768, 2003.

**APPENDIX A: ADDITIONAL DATA**

Table A.1. GPC result of the crosslinker.

Compound	GPC result (Mn)
PEG-bisacid	$7.4877 \cdot 10^3$
Furan Protected Bismaleimide Crosslinker	$1.3845 \cdot 10^4$
Bismaleimide Crosslinker	$9.4992 \cdot 10^3$

Table A.1. GPC result of the crosslinker

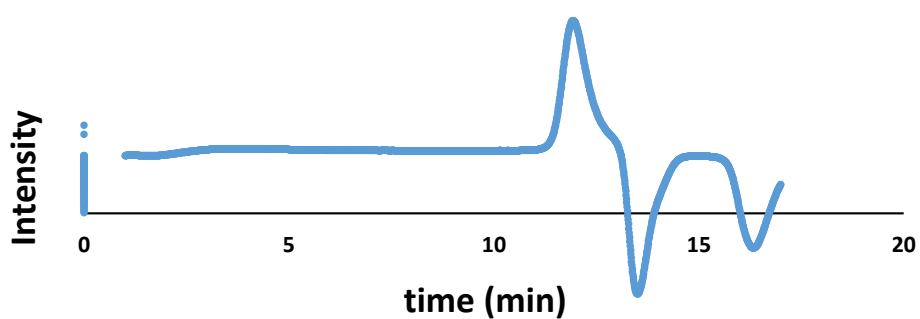


Figure A.1. GPC plot of PEG. (Mw=4kDa)

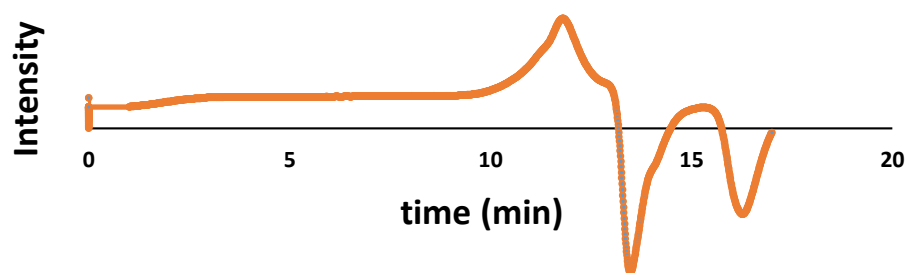


Figure A.2. GPC plot of furan protected bismaleimide crosslinker.

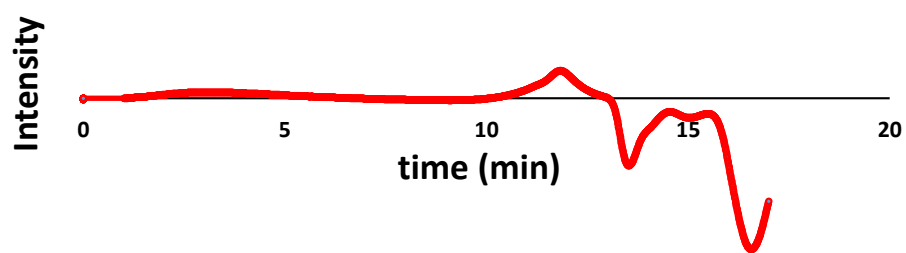


Figure A.3. GPC plot of bismaleimide crosslinker.

## APPENDIX B: COPYRIGHTS

### Order Completed

Thank you for your order.  
This Agreement between Bogaziçi University – Yagmur Bas ("You") and John Wiley and Sons ("John Wiley and Sons") consists of your license details and the terms and conditions provided by John Wiley and Sons and Copyright Clearance Center.

Your confirmation email will contain your order number for future reference.

License Number 4720250152747 [Printable Details](#)

License date Dec 01, 2019

Licensed Content		Order Details	
Licensed Content Publisher	John Wiley and Sons	Type of use	Dissertation/Thesis
Licensed Content Publication	Advanced Materials Technologies	Requestor type	University/Academic
Licensed Content Title	Transformer Hydrogels: A Review	Format	Electronic
Licensed Content Author	David H. Gracias, Wangyu Liu, Akhweya Pantula, et al	Portion	Figure/table
Licensed Content Date	Feb 27, 2019	Number of figures/tables	1
Licensed Content Volume	4	Will you be translating?	No
Licensed Content Issue	4		
Licensed Content Pages	27		

About Your Work		Additional Data	
Title of your thesis / dissertation	Novel Hydrogels for Wound Care Applications	Original Wiley figure/table number(s)	1
Expected completion date	Jan 2020		
Expected size (number of pages)	70		

Requestor Location

Bogaziçi University  
Ayçi İplik, Parklar-İst. No:20-22  
dare-5 Koçuyolu/İstanbul

Requestor Location  
Istanbul, Istanbul 34742  
Turkey  
Atm: Bogaziçi University

Requestor Tax ID  
EUB26007151

Price

Total 0.00 USD

Thank you for your order.  
This Agreement between Bogaziçi University – Yagmur Bas ("You") and John Wiley and Sons ("John Wiley and Sons") consists of your license details and the terms and conditions provided by John Wiley and Sons and Copyright Clearance Center.

Your confirmation email will contain your order number for future reference.

License Number 4720250640554 [Printable Details](#)

License date Dec 01, 2019

Licensed Content		Order Details	
Licensed Content Publisher	John Wiley and Sons	Type of use	Dissertation/Thesis
Licensed Content Publication	Advanced Materials	Requestor type	University/Academic
Licensed Content Title	Hyaluronic Acid Hydrogels for Biomedical Applications	Format	Print and electronic
Licensed Content Author	Glen D. Preston, Jason A. Burdick	Portion	Figure/table
Licensed Content Date	Mar 10, 2011	Number of figures/tables	1
Licensed Content Volume	23	Will you be translating?	No
Licensed Content Issue	12		
Licensed Content Pages	16		

About Your Work		Additional Data	
Title of your thesis / dissertation	Novel Hydrogels for Wound Care Applications	Original Wiley figure/table number(s)	1
Expected completion date	Jan 2020		
Expected size (number of pages)	70		

Requestor Location

Bogaziçi University  
Ayçi İplik, Parklar-İst. No:20-22  
dare-5 Koçuyolu/İstanbul

Requestor Location  
Istanbul, Istanbul 34742  
Turkey  
Atm: Bogaziçi University

Requestor Tax ID  
EUB26007151

Price

Total 0.00 USD



RightsLink®

Home ? Email Support Yagmur Bas v

### Novel Hydrogels via Click Chemistry: Synthesis and Potential Biomedical Applications

Author: Vittorio Crescenzi, Lisa Cornelio, Chiara Di Meo, et al



Publication: Biomacromolecules

Publisher: American Chemical Society

Date: Jun 1, 2007

Copyright © 2007, American Chemical Society

#### PERMISSION/LICENSE IS GRANTED FOR YOUR ORDER AT NO CHARGE

This type of permission/license, instead of the standard Terms & Conditions, is sent to you because no fee is being charged for your order. Please note the following:

- Permission is granted for your request in both print and electronic formats, and translations.
- If figures and/or tables were requested, they may be adapted or used in part.
- Please print this page for your records and send a copy of it to your publisher/graduate school.
- Appropriate credit for the requested material should be given as follows: "Reprinted (adapted) with permission from (COMPLETE REFERENCE CITATION). Copyright (YEAR) American Chemical Society." Insert appropriate information in place of the capitalized words.
- One-time permission is granted only for the use specified in your request. No additional uses are granted (such as derivative works or other editions). For any other uses, please submit a new request. If credit is given to another source for the material you requested, permission must be obtained from that source.

[BACK](#)

[CLOSE WINDOW](#)

Thank you for your order.  
This Agreement between Bogaziçi University – Yagmur Bas ("You") and Elsevier ("Elsevier") consists of your license details and the terms and conditions provided by Elsevier and Copyright Clearance Center.

Your confirmation email will contain your order number for future reference.

License Number: 4720260793931 [Printable Details](#)

License date: Dec 01, 2019

Licensed Content		Order Details	
Licensed Content Publisher	Elsevier	Type of Use	reuse in a thesis/dissertation
Licensed Content Publication	Biomaterials Hyaluronic acid-based hydrogels functionalized with heparin that support controlled release of bioactive BMP-2	Portion	figures/tables/illustrations
Licensed Content Title	Gaoshan B,Shen B,He N,Chen X,K,Lin J,James H, Hu, Gary S, Stein, Andre J, van Wijnen,Victor N,urcombe Glenn D, Prestwich,Simon M, Cool	Number of figures/tables/illustrations	1
Licensed Content Author	Sep 1, 2012	Format	both print and electronic
Licensed Content Date	33	Are you the author of this Elsevier article?	No
Licensed Content Volume	26	Will you be translating?	No
Licensed Content Issue	13		
Licensed Content Pages	S&T		
Licensed Content Journal Type			
About Your Work		Additional Data	
Title	Novel Hydrogels for Wound Care Applications	Portions	Fig 2.
Institution name	n/a		
Expected presentation date	Jan 2020		
Requestor Location		Tax Details	
Requestor Location	Bogaziçi University Ayçi sok. Perihan apt. No:20-22 cahne S Kocayatağı/Istanbul	Publisher Tax ID	GB 494 6272 12
	Istanbul, Istanbul 34742 Turkey Atm: Bogaziçi University		
\$ Price			
Total	0.00 USD		

Thank you for your order.  
This Agreement between Bogaziçi University – Yagmur Bas ("You") and Elsevier ("Elsevier") consists of your license details and the terms and conditions provided by Elsevier and Copyright Clearance Center.

Your confirmation email will contain your order number for future reference.

License Number: 4720260978510 [Printable Details](#)

License date: Dec 01, 2019

Licensed Content		Order Details	
Licensed Content Publisher	Elsevier	Type of Use	Reuse in a thesis/dissertation
Licensed Content Publication	Acta Biomaterialia Characterization of glycidyl methacrylate - Crosslinked hyaluronan hydrogel scaffolds incorporating elastogenic hyaluronan oligomers	Portion	figures/tables/illustrations
Licensed Content Title	S. Ibrahim,C.R. Kocapalli,Q.K. Kang,A. Ramamurthi	Number of figures/tables/illustrations	1
Licensed Content Author	Feb 1, 2011	Format	both print and electronic
Licensed Content Date	7	Are you the author of this Elsevier article?	No
Licensed Content Volume	2	Will you be translating?	No
Licensed Content Issue	13		
Licensed Content Pages	S&T		
Licensed Content Journal Type			
About Your Work		Additional Data	
Title	Novel Hydrogels for Wound Care Applications	Portions	Fig 1.
Institution name	n/a		
Expected presentation date	Jan 2020		
Requestor Location		Tax Details	
Requestor Location	Bogaziçi University Ayçi sok. Perihan apt. No:20-22 cahne S Kocayatağı/Istanbul	Publisher Tax ID	GB 494 6272 12
	Istanbul, Istanbul 34742 Turkey Atm: Bogaziçi University		
\$ Price			
Total	0.00 USD		



RightsLink®

Home ? Email Support Yagmur Bas v



### Diels-Alder Click Cross-Linked Hyaluronic Acid Hydrogels for Tissue Engineering

Author: Chelsea M. Nimmo, Shawn C. Owen, Molly S. Shoichet

Publication: Biomacromolecules

Publisher: American Chemical Society

Date: Mar 1, 2011

Copyright © 2011, American Chemical Society


#### PERMISSION/LICENSE IS GRANTED FOR YOUR ORDER AT NO CHARGE

This type of permission/license, instead of the standard Terms & Conditions, is sent to you because no fee is being charged for your order. Please note the following:

- Permission is granted for your request in both print and electronic formats, and translations.
- If figures and/or tables were requested, they may be adapted or used in part.
- Please print this page for your records and send a copy of it to your publisher/graduate school.
- Appropriate credit for the requested material should be given as follows: Reprinted (adapted) with permission from (COMPLETE REFERENCE CITATION). Copyright (YEAR) American Chemical Society. Insert appropriate information in place of the capitalized words.
- One-time permission is granted only for the use specified in your request. No additional uses are granted (such as derivative works or other editions). For any other uses, please submit a new request.
- If credit is given to another source for the material you requested, permission must be obtained from that source.


BACK

CLOSE WINDOW

 **RightsLink** [Home](#) [?](#) [Help](#) [Email Support](#) [Yagmur Bas](#) v

---

**Injectable Click-Crosslinked Hyaluronic Acid Depot To Prolong Therapeutic Activity in Articular Joints Affected by Rheumatoid Arthritis**

 Author: Jyoung Seo, Seung Hun Park, Min Ju Kim, et al  
Publication: Applied Materials  
Publisher: American Chemical Society  
Date: Jul 1, 2019  
Copyright © 2019, American Chemical Society

---

**PERMISSION/LICENSE IS GRANTED FOR YOUR ORDER AT NO CHARGE**

This type of permission/license, instead of the standard Terms & Conditions, is sent to you because no fee is being charged for your order. Please note the following:

- Permission is granted for your request in both print and electronic formats, and translations.
- If figures and/or tables were requested, they may be adapted or used in part.
- Please print this page for your records and send a copy of it to your publisher/graduate school.
- Appropriate credit for the requested material should be given as follows: "Reprinted (adapted) with permission from (COMPLETE REFERENCE CITATION). Copyright (YEAR) American Chemical Society." Insert appropriate information in place of the capitalized words.
- One-time permission is granted only for the use specified in your request. No additional uses are granted (such as derivative works or other editions). For any other uses, please submit a new request. If credit is given to another source for the material you requested, permission must be obtained from that source.

[BACK](#) [CLOSE WINDOW](#)

